AN ABSTRACT OF THE THESIS OF

YIN-SANG SHUM (Name) for the MASTER OF SCIENCE (Degree)

in CHEMISTRY (Major) presented on JULY 13, 1971 (Date)

Title: ISOMERIC CROSS-SECTION RATIOS OF Cd^{115} AND Cs^{134} FOR CHARGED PARTICLE INDUCED FISSION

Redacted for Privacy

Abstract approved: Walter D. Loveland

The isomer yield ratios of Cd^{115m}(J, π = 11/2-) to Cd^{115g}(J, π = 1/2-) and Cs^{134m}(J, π = 8-) to Cs^{134}g(J, π = 4+) have been investigated for the reactions U^{238}(35 MeV α, f), Bi^{209}(35 MeV α, f) Ra^{226}(19 MeV d, f), and Th^{232}(20 MeV d, f). After the bombardments, radiochemical separation techniques were used to separate the Cd and Cs isotopes from the fission products. The gamma-ray lines (observed with a Ge(Li) detector) used to measure the abundance of the radionuclides were: Cs^{134m}, 128 keV; Cs^{134g}, 796 and 808 keV; Cd^{115m}, 935 keV and Cd^{115g}, 335 keV. The values of the Cd isomer ratio were 0.048 ± 0.05, 0.063 ± 0.010, 0.98 ± 0.13 and 0.90 ± 0.20 for the fission of U^{238}, Th^{232}, Ra^{226} and Bi^{209} respectively. The values of the Cs isomer ratio were 0.53 ± 0.06, 0.57 ± 0.05 and 0.22 ± 0.12 for fission of U^{238}, Th^{232} and Ra^{226} respectively.

With the application of statistical theory and the formalism developed by Vandenbosch and Huizenga (1), the initial average angular momenta of the primary fission fragments were deduced. One concludes that:

1. The magnitude of the average fragment angular momentum in charged particle induced fission is greater than or equal to the average fragment angular momentum in low energy induced or spontaneous fission.
2. There appears to be no correlation between the angular momentum of the initial compound nucleus formed in fission and the fragment angular momentum.
3. As the (Z, A) of the fissioning system decrease, the average fragment angular momentum increases.

Isomeric Cross-Section Ratios of Cd^{115} and Cs^{134} for Charged Particle Induced Fission

by

Yin-Sang Shum

A THESIS

submitted to

Oregon State University

in partial fulfillment of
the requirements for the
degree of

Master of Science

June 1972

APPROVED:

Redacted for Privacy

Assistant Professor of Chemistry

in charge of major

Redacted for Privacy

Head of Department of Chemistry

Redacted for Privacy

Dean of Graduate School

Date thesis is presented July 13, 1971

Typed by Barbara Eby for Yin-Sang Shum

ACKNOWLEDGMENTS

The author wishes to express his gratitude to Dr. Walter D. Loveland, for his help, guidance, encouragement and for the A. E. C. research assistantship throughout the course of this work.

The author also wishes to thank Dr. Roman A. Schmitt for his helpful suggestions regarding radiochemical separations.

The cooperation of the personnel of the 60 inch cyclotron group at the University of Washington is gratefully acknowledged.

TABLE OF CONTENTS

LIST OF TABLES

LIST OF FIGURES

ISOMERIC CROSS-SECTION RATIOS OF Cd^{115} AND Cs^{134} FOR CHARGED PARTICLE INDUCED FISSION

INTRODUCTION

In the study of nuclear fission, it is assumed that the target nucleus, after interacting with a projectile, forms a compound nucleus. This nucleus first deforms to the saddle point, then the scission point. This phenomenon is called nuclear fission.

The study of the mechanism of the actual splitting of the nucleus is one of the most important subjects in the overall study of nuclear fission. Detailed knowledge of this process, called the scission stage, is not available. One way to obtain this kind of information is to find out the average initial angular momenta carried by the primary fission fragments. This can provide us with some information on the dynamics in the break-up process in nuclear fission.

From the measurement of the fission product isomeric cross-section ratio which is defined as the ratio of the cross-section for the formation of a fission product nuclide in a metastable state to the formation cross-section for the same nucleus in its ground state, one can deduce the average initial fragment angular momenta by use of statistical theory of nuclear reactions.

Such isomer ratios are measured for a typical symmetric fission product, Cd^{115}, and a typical asymmetric fission product, Cs^{134} for

the following cases of charged particle induced fission: U^{238} (35 Mev α, f) Th^{232} (20 MeV d, f), Ra^{226} (19 MeV d, f) and Bi^{209} (35 MeV α, f).

EXPERIMENTAL PROCEDURE

Preparation of Targets

In the preparation of U^{238} target, the thin film technique developed by K. M. Glover and P. Borrell (2) was applied. An alcoholic solution of uranium nitrate was mixed with a 3 per cent solution of cellulose nitrate prepared by dissolving celluloid in amyl acetate and the resulting solution diluted with acetone. The solution was then spread over the backing material (aluminum foil), dried and ignited to remove the organic substances.

For the preparation of radium target, similar method as for U^{238} target was applied. Twenty milligrams of radium chloride was used with the precaution that the experiment should be done in a glove box to avoid contamination and the spread of radon.

The Bi^{209} target was purchased from A. D. Mackay Inc. in Broadway, New York with 99.99% purity.

The Th^{232} target was a gift of the U. S. Bureau of Mines in Albany, Oregon.

The target thicknesses ranged from 2 to 5 mg./cm.^{2}

Irradiation Procedure

The target was mounted on a target plate as shown in Figure 1 and was covered with pure aluminum foil which acted as catcher foil

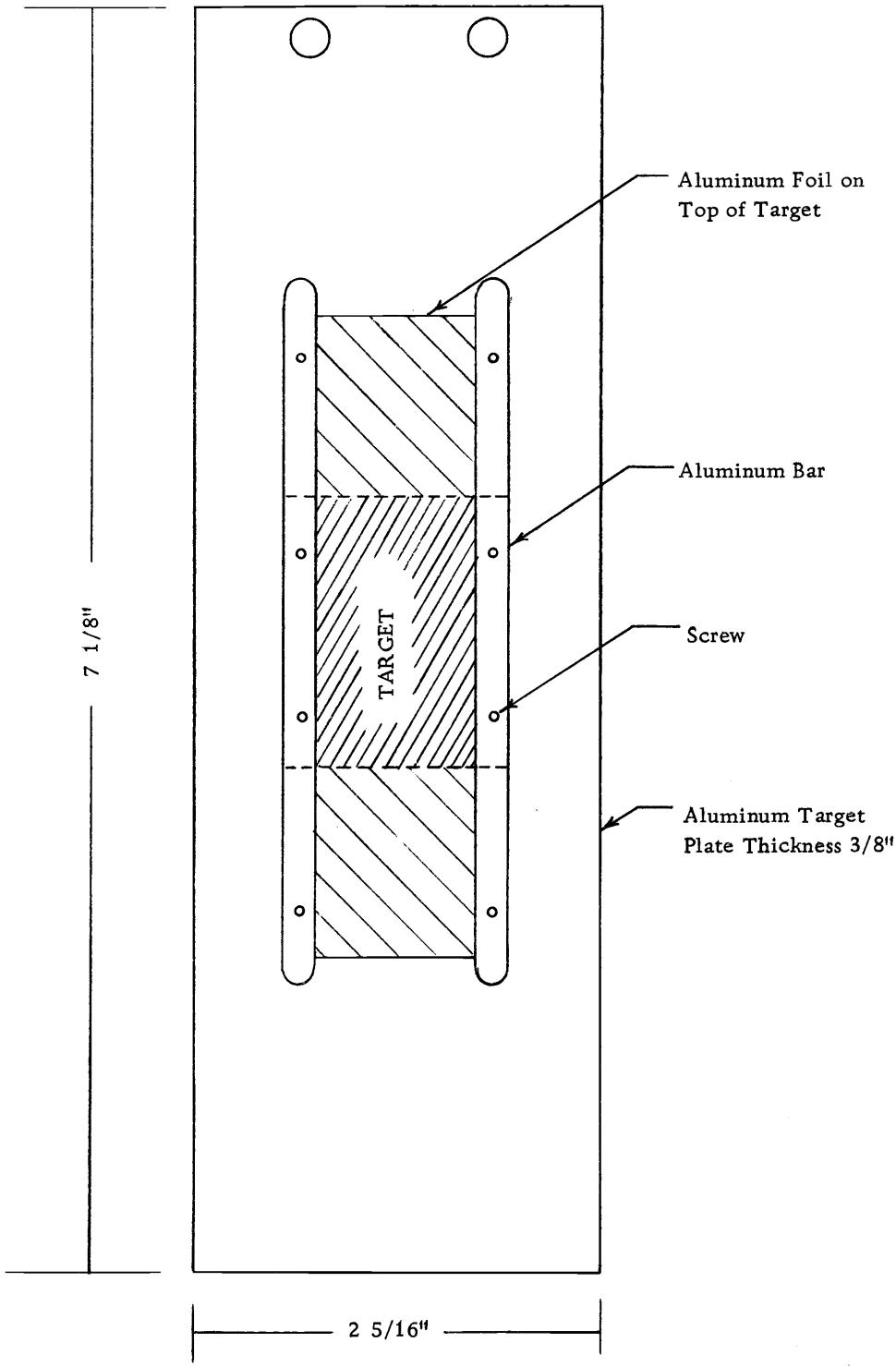

Figure 1. Target plate for foil target.

for the fission products. By bombarding a blank aluminum foil alone, it was shown that no disturbing activity was produced in the catcher foil. The target plate was inserted in a target box as shown in Figure 2 and was irradiated in the external beam of the 60 inch cyclotron of the University of Washington. The irradiation time was about two hours for the cases of U^{238} and Th^{232} fission and about four hours for the cases of Ra^{226} and Bi^{209} fission. For the case of radium, the target was completely sealed by sandwiching with two more aluminum plates as shown in Figure 3. This is to minimize the amount of radon leaking out during irradiation of the target. For the bombardment by deuterons and alpha particles, the beam current was about 25 micro-amperes.

Radiochemical Separation

At the end of bombardment, the target was allowed to cool for about half to one hour. The target foil and the aluminum catcher foil were removed from the target plate. Both foils were dissolved in about 40 c. c. of 6N HCl for the cases of U^{238}, Bi^{209} and Th^{232} fission. For the case of Ra^{226} fission, only the catcher foil was dissolved.

For the radiochemical separation of Cd, the dithizone method was used (3). An aliquot of 15 c. c. of the fission product solution was pipeted into a 100 ml. beaker and to which 0. 2 gm. solid sodium tartrate was added. The pH of the solution was adjusted to 13-13. 5

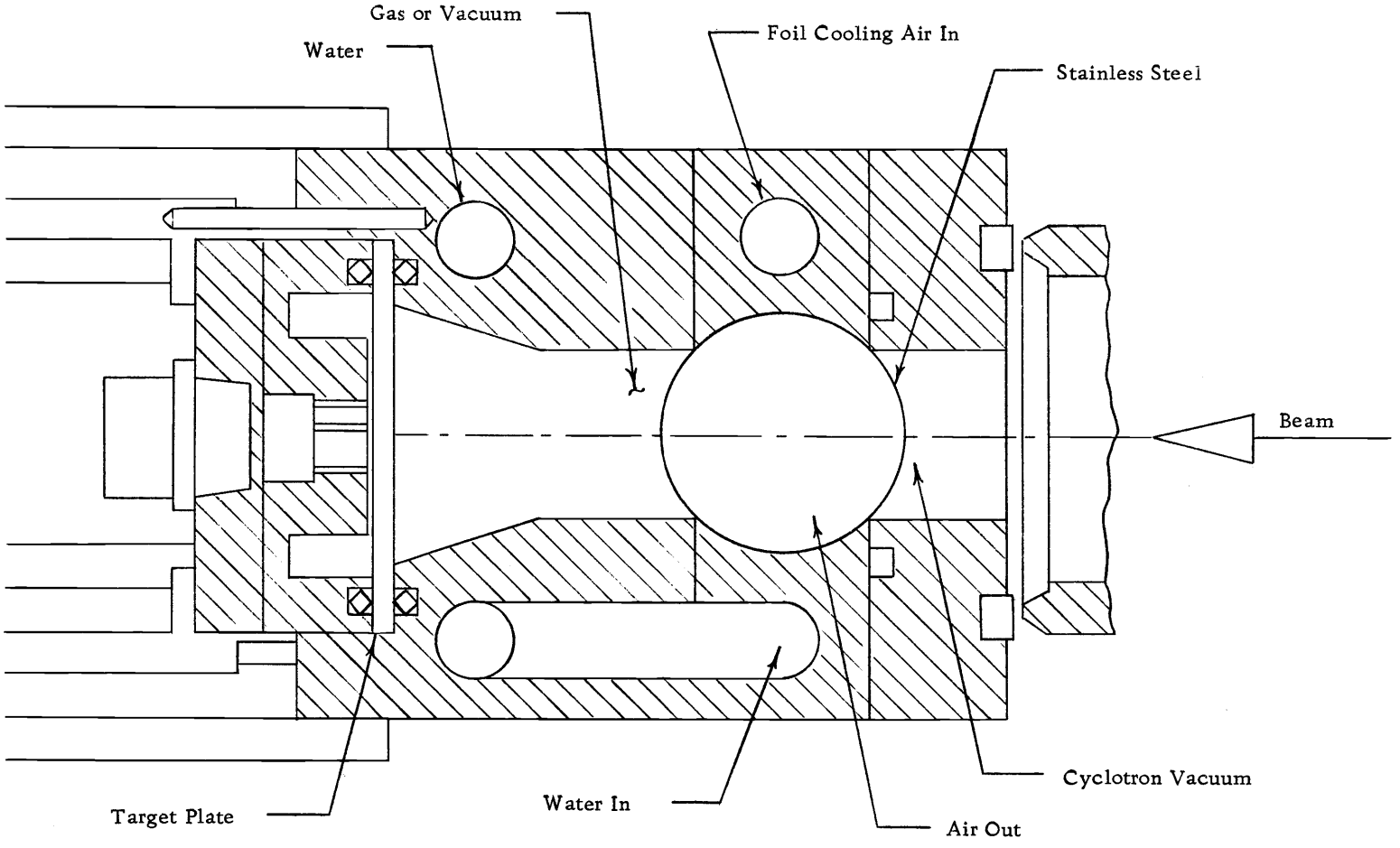

Figure 2. Foil target window and target holder assembly.

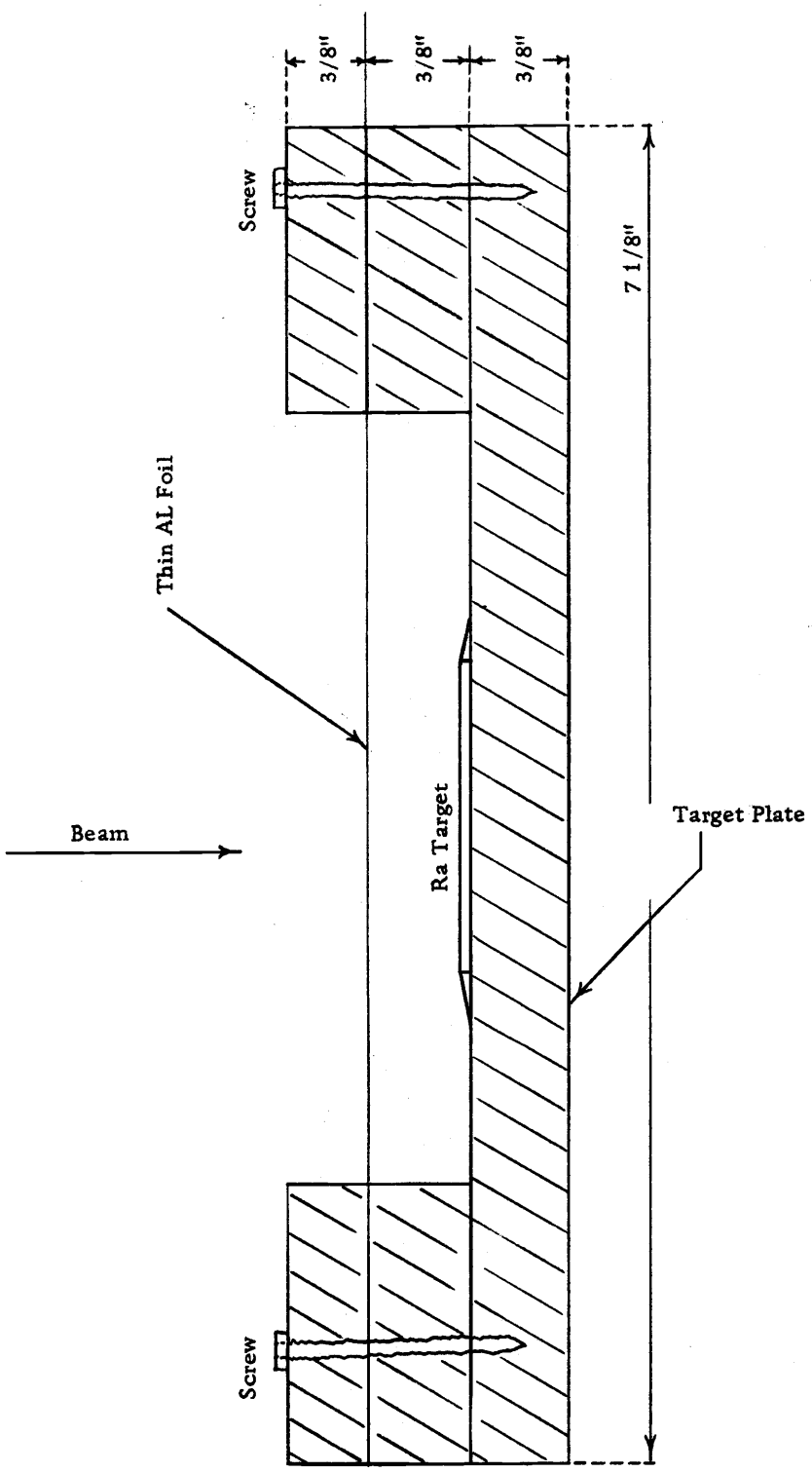

Figure 3. Target plate assembly for Ra fission.

with 6N sodium hydroxide. The solution was then transferred to a separating funnel containing 15 ml. of dithizone solution (0.75 mg./ml.) in chloroform and stirred rapidly for two minutes. The chloroform layer was drawn off into exactly 10 ml. of 0.1 M hydrochloric acid and was stirred rapidly for two minutes. The acid layer was removed into a polyvial container and the sample was ready for counting purposes. The chemical yield of this process is about 77%. The time for this separation is about 15 minutes.

For the chemical separation of Cs, the perchlorate method was applied (4). 15 ml. of the fission product solution was transferred to a 50 ml. centrifuge tube and into which 2 ml. of Cs carrier (ca. 25 mg. CsCl), 5 ml. of 70% $HClO_4$ were added. The solution was then evaporated until dense white $HClO_4$ fumes evolved. The solution was cooled and stirred until white precipitate occurred. The precipitate was centrifuged down and washed two times with 10 ml. absolute ethanol. The precipitate was then dissolved in 10 ml. of water, heated to incipient boiling and 5 mg. Fe^{+3} carrier was added. $Fe(OH)_3$ was precipitated by adding 6N NH_4OH dropwise to the solution. The solution was centrifuged and the precipitate discarded. The precipitation was repeated by adding 5 mg. Fe^{+3} carrier and the precipitate discarded. Five drops of 6N NaOH were added to the solution and the solution was evaporated to a total volume of 5 ml. Four ml. of 70% $HClO_4$ was added to the solution which was then evaporated by swirling

over a burner until $HClO_4$ fumes appeared. The solution was cooled and 15 ml. of absolute ethanol was added and stirred until white precipitate of cesium perchlorate appeared. The precipitate was filtered onto a weighed filter paper in a small Hirsch funnel and mounted on a card and covered by scotch tape for counting purposes.

Sample Counting

After radiochemical separation, the samples were counted by a 30 c. c. Ge(Li) detector to measure the gamma ray spectra as a function of time. A Ge(Li) detector was chosen instead of a NaI(Tl) detector because of its good resolution. A block diagram of the counting set-up is shown in Figure 4. When the gamma radiation enters the Ge(Li) detector, the output voltage pulse is amplified by the preamplifier and amplifier and analyzed by a multichannel analyzer. The use of Ge(Li) detector in gamma ray spectroscopy has been treated in detail by many authors (5-7). Therefore, further discussion on the use of a single crystal for gamma ray detection will not be given here.

Determination of Absolute Efficiency of Detector

Since the calculation of the isomeric cross-section ratio requires the knowledge of absolute disintegration rate, one has to know the absolute photopeak efficiency of the detector at the same geometry where the sample was counted. The absolute photopeak efficiency of a

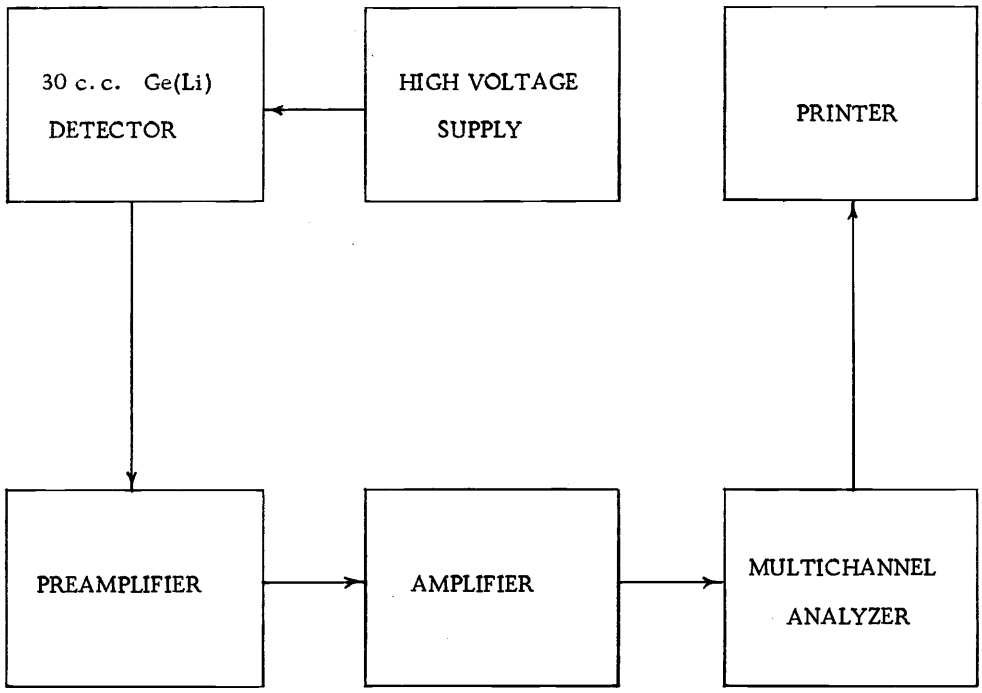

Figure 4. Setup of sample counting.

detector is defined as $E_{abs.} = A/(D \times F)$ where A is the net count rate of the photopeak (counts per second), F is the γ-ray branching ratio and D is the total up-to-date disintegration rate of the source used for the measurement (counts per second).

The absolute efficiency of the detector was determined using a set of standard disk sources from Nuclear Associates, Inc. The source strengths and the fraction of decay of the photopeaks are listed as follows:

Source	Strength	Date	E(MeV)	Fraction of Decay[8]
Co^{57}	1.65 uc	8/20/69	0.122	87%
Na^{22}	1.03 uc	12/9/68	0.511	180% (β^+ emitter)
			1.275	100%
Cs^{137}	1.10 uc	12/9/68	0.662	85%
Mn^{54}	1.36 uc	8/22/69	0.835	100%
Co^{60}	1.18 uc	12/9/68	1.173	100%
			1.332	100%

Therefore, from the above equation and information, one can determine the absolute efficiency of the detector as a function of energy at a fixed geometry. The absolute efficiency of a 30 c. c. Ge(Li) detector as a function of energy at various geometry are shown in Figure 5.

Later on, a set of more accurate standard sources from International Atomic Energy Association (I. A. E. A.) was used. It was found that the absolute photopeak efficiencies calculated were the

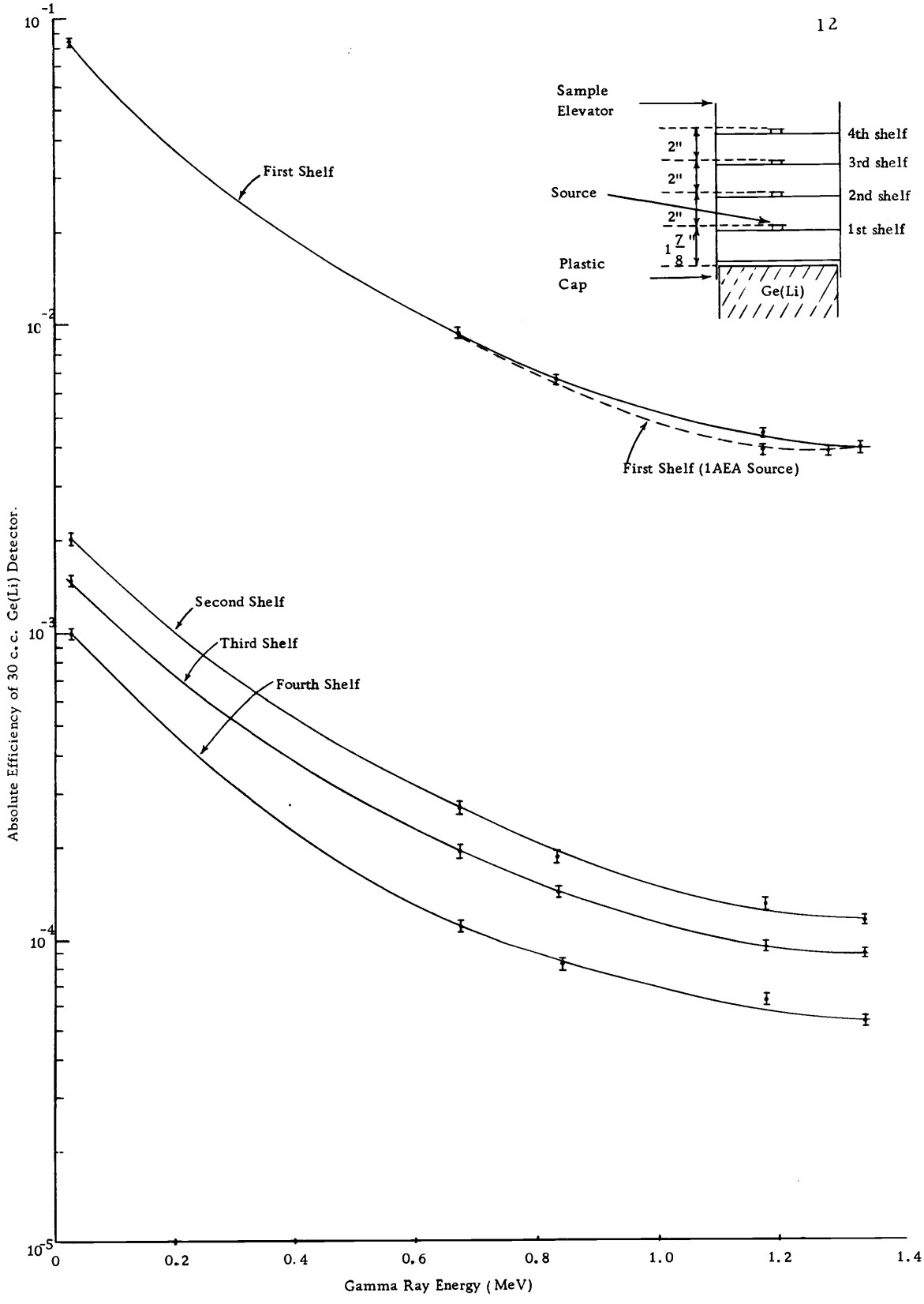

Figure 5. Absolute efficiency of 30 c.c (GeLi) detector.

same as the N. A. I. disk source for gamma energy from 0. 122 MeV to 0. 835 MeV and a very small difference from 0. 835 MeV to 1. 33 MeV as shown in Figure 5. Therefore, the calculations for the isomer ratios are based on the absolute photopeak efficiencies by using the I. A. E. A. sources.

Counting of the Isomers

Cs^{134m}. The cesium 134 metastable state has a half life of 2. 91 hours and its decay scheme (8) is shown in Figure 6. Since this isomer has a short half-life, it should be counted immediately after radiochemical separation. The intensity of the gamma ray line at 0. 128 MeV was measured as a function of time for a period of about 8 hours until its half-life was identified. The counts in the region of the 0. 128 MeV peak were integrated and plotted versus time.

Besides the Cs^{134} isomers in the sample, there are other cesium isotopes produced with a large yield in the medium energy fission (9). Among these are: 52 minute Cs^{135m}, 13 day Cs^{136} and 32 minute Cs^{138}. They contribute strongly to the gamma spectrum of the sample. The most interferring isotope for the measurement of Cs^{134m} isomer was Cs^{136} which has gamma ray peaks at 0. 067, 0. 086 and 0. 16 MeV.

Therefore, due to the high background at low gamma energies and the above interferring peaks, it is advantageous to use a Ge(Li) detector for the measurement of the 0. 128 MeV peak. It was found

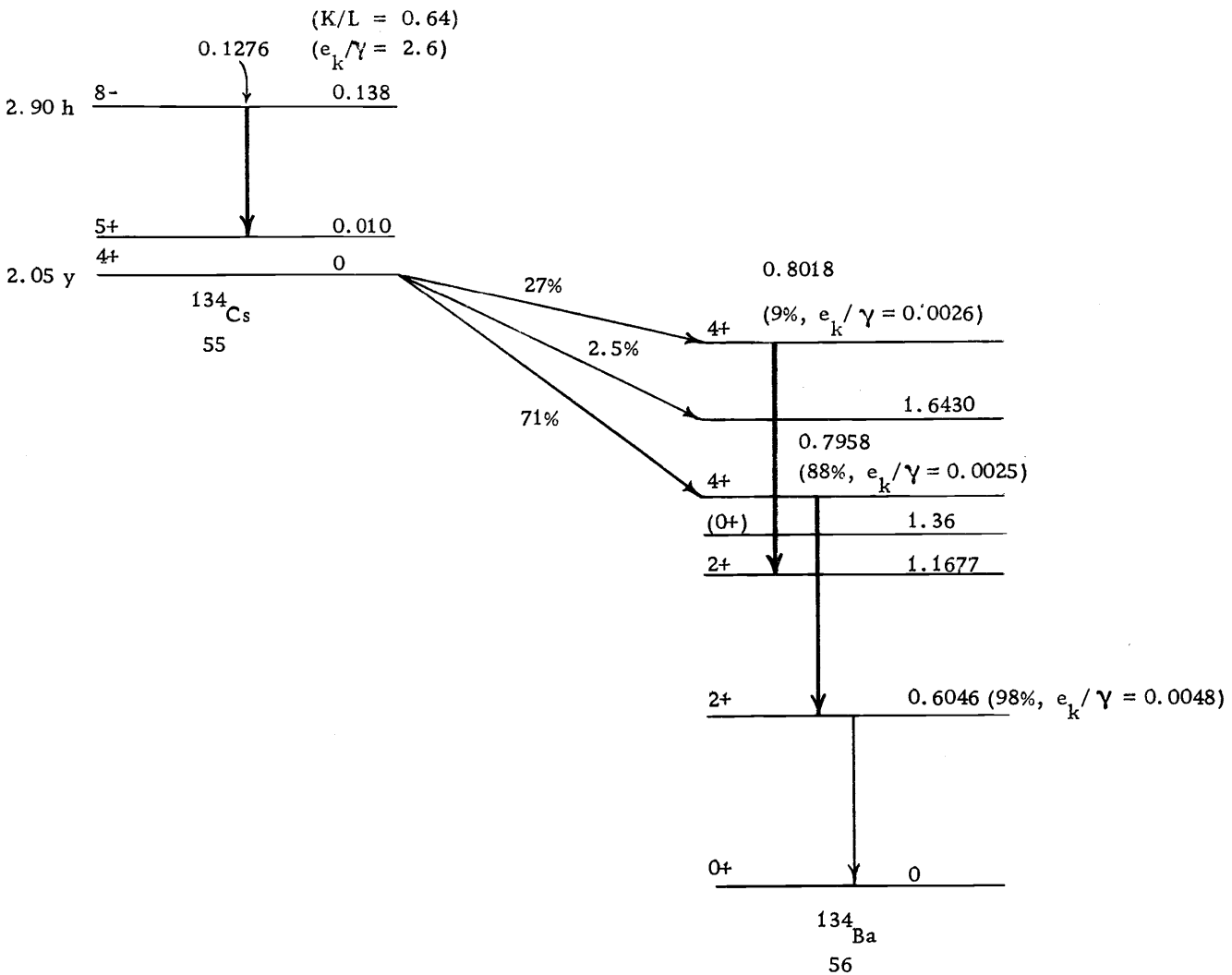

Figure 6. Decay scheme of Cs^{134}.

that a 30 c. c. detector could resolve all these peaks without any significant interferences.

Cs^{134g}. The cesium 134 ground state has a half-life of 2.05 years and its decay scheme (8) is shown in Figure 6. The intensity of the gamma ray lines at 0.796 and 0.801 MeV were measured after letting the sample to decay for about four months such that the 13 day Cs^{136} had decayed sufficiently to give negligible contribution to the measured activities. About two weeks was required for each counting because the activity was very low.

Cd^{115m}. The half-life of Cd 115 metastable state is 43 days and its decay scheme (8) is shown in Figure 7. The intensity of the gamma ray line at 0.935 MeV was measured for a period of about 3 to 4 days. The sample was recounted for every two weeks until its half-life was identified.

Cd^{115g}. The half-life of Cd 115 ground state is 53.5 hours and its decay scheme (8) is shown in Figure 7. The intensity of the gamma ray line at 0.335 MeV was measured in one or two days after radiochemical separation and for every day afterwards until its half-life was identified.

One comment should be made in obtaining the net counting rate of the photopeak. Since the photopeak to be measured was of low activity and the background was high, one has to be very careful in evaluation of the activity due to Compton effect. In this case, one cannot use only

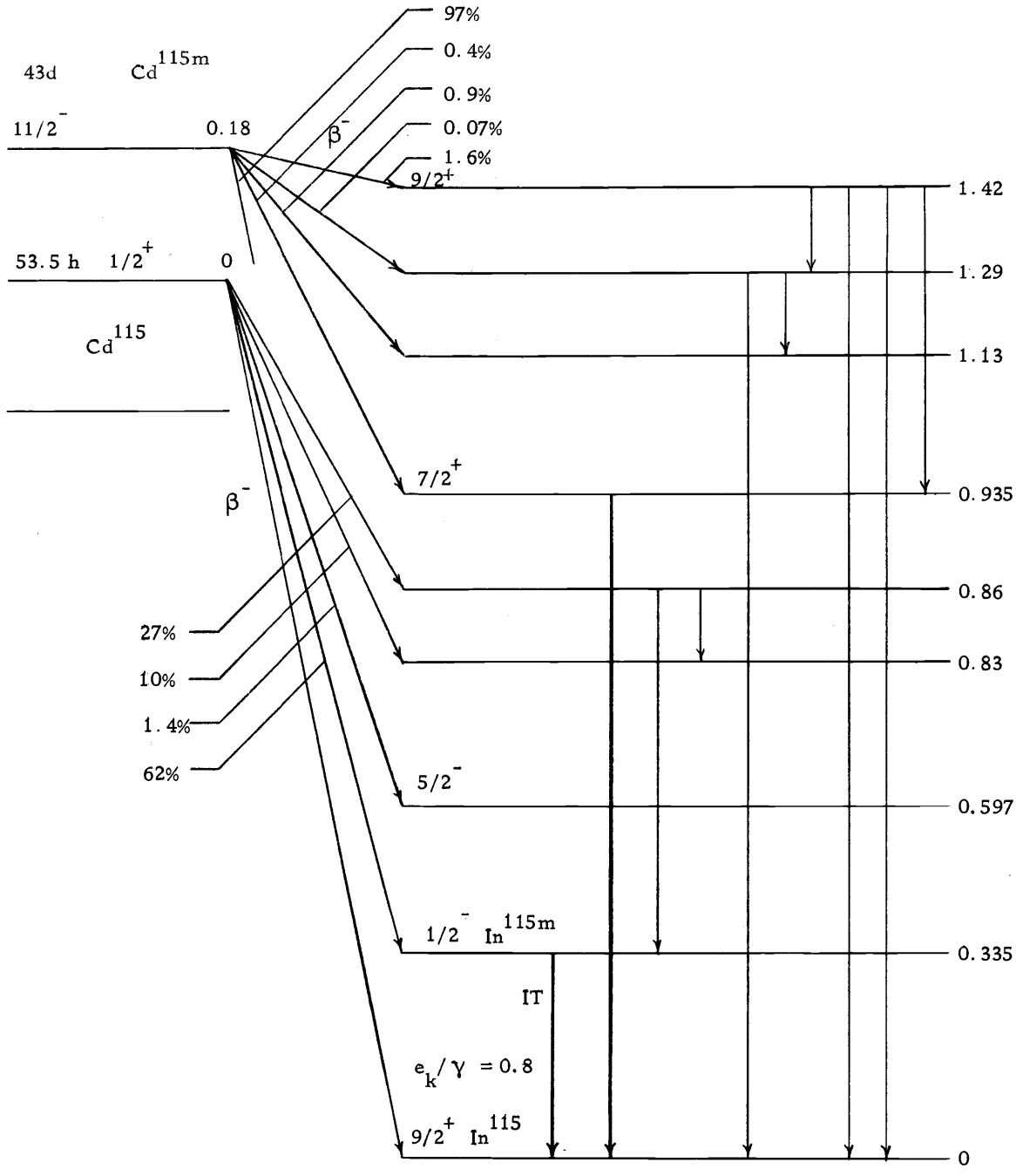

Figure 7. Decay scheme of Cd^{115}.

two points to form the base line for the usual Compton effect calculations; one has to average several points at the base of the photopeak in order to obtain an average value due to Compton contribution.

Calculation of Experimental Isomer Ratio

In the calculation of the experimental cross-section for the metastable state, one has to solve the rate equation for the formation of this nuclide produced at a constant rate. For a thin target and a constant flux, the rate of change of the number of the metastable state atoms dN_m/dt is given by

$$dN_m/dt = R_m - \lambda_m N_m \tag{2.1}$$

where R_m is the rate of formation of the metastable state atoms, $\lambda_m N_m$ is its rate of decay. R_m is given by

$$R_m = nf\sigma_m \tag{2.2}$$

where n is the number of target atoms and σ_m is the cross-section of formation of the metastable state and f is the flux of the bombarding particles.

The solution of Equation (2.1) is given by

$$\lambda_m N_m = nf\sigma_m(1 - e^{-\lambda_m t_i}) \tag{2.3}$$

where t_i is the time of irradiation, $\lambda_m N_m$ is the absolute

disintegration rate after an irradiation time t_i. Therefore, from Equation (2. 3),

$$\sigma_m = \lambda_m N_m / nf(1 - e^{-\lambda_m t_i}) \qquad (2.4)$$

Suppose the activity of the metastable state is measured at time t_m after the end of bombardment and its absolute activity is $A_m^{t_m}$, then $\lambda_m N_m$ is given by

$$\lambda_m N_m = A_m^{t_m} e^{\lambda_m t_m} \qquad (2.5)$$

Substituting Equation (2. 4) in (2. 5), therefore,

$$\sigma_m = A_m^{t_m} e^{\lambda_m t_m} / (1 - e^{\lambda_m t_i}) nf \qquad (2.6)$$

where $A_m^{t_m}$ is equal to the net photopeak rate at t_m divided by the product of the absolute photopeak efficiency of the detector and the branching ratio of the gamma ray line measured.

For the calculation of the experimental cross-section for the ground state, the procedure is more complicated because the decay of the metastable to the ground state during the irradiation has to be taken into account. Therefore, the rate of change of the number of the ground state is given by

$$dN_g/dt = R_g + N_m \lambda_m - N_g \lambda_g \qquad (2.7)$$

where R_g is the rate of formation of the ground state nuclide, $N_m \lambda_m$

is the rate of growth of ground state nuclei from the metastable state and $N_g \lambda_g$ is the rate of decay of the ground state.

Substituing Equation (2. 4) into Equation (2. 7) and rearranging, we have

$$dN_g/dt + \lambda_g N_g = R_g + R_m - R_m e^{-\lambda_m t_i} \qquad (2.8)$$

In order to solve Equation (2. 8), the reduced equation

$$dN_g/dt + \lambda_g N_g = 0 \qquad (2.9)$$

has to be solved first and add it to a particular solution of Equation (2. 8).

The solution of Equation (2. 9) is given by

$$N_g = Ce^{-\lambda_g t_i} \qquad (2.10)$$

Suppose we assume a particular solution of 2. 8 and let

$$N_g = ae^{-\lambda_m t_i} + b \qquad (2.11)$$

where a and b are to be determined.

Differentiating Equation (2. 11) with respect to t , we obtain

$$dN_g/dt = -a\lambda_m e^{-\lambda_m t_i} \qquad (2.12)$$

By equating (2. 8), (2. 11) and (2. 12) we have

$$-a\lambda_m e^{-\lambda_m t_i} + \lambda_g a e^{-\lambda_m t_i} + \lambda_g b = R_g + R_m - R_m e^{-\lambda_m t_i} \tag{2.13}$$

Also by equating coefficients, we have

$$-a\lambda_m + a\lambda_g = -R_m \tag{2.14}$$

$$a = R_m/(\lambda_m - \lambda_g) \tag{2.15}$$

$$\lambda_g b = R_g + R_m \tag{2.16}$$

$$b = (R_g + R_m)/\lambda_g \tag{2.17}$$

Therefore, Equation (2. 11) becomes

$$N_g = (R_m/(\lambda_m - \lambda_g))e^{-\lambda_m t_i} + (R_g + R_m)/\lambda_g \tag{2.18}$$

Comparing Equation (2. 10) and Equation (2. 18), Equation (2. 8) becomes

$$N_g = Ce^{-\lambda_g t_i} + (R_m/(\lambda_m - \lambda_g))e^{-\lambda_m t_i} + (R_g + R_m)/\lambda_g \tag{2.19}$$

The coefficient C can be determined by assuming at zero time, that $N_g = 0$. Therefore, C is equal to

$$C = -R_m/(\lambda_m - \lambda_g) - (R_g + R_m)/\lambda_g \tag{2.20}$$

Equation (2. 19) then becomes

$$\lambda_g N_g = (R_m + R_g)(1 - e^{-\lambda_g t_i}) + \lambda_g R_m (e^{-\lambda_m t_i} - e^{-\lambda_g t_i})/(\lambda_m - \lambda_g) \tag{2. 21}$$

By substituting $R_m = nf\sigma_m$ and $R_g = nf\sigma_g$ into Equation (2. 21) and rearranging, it becomes

$$\lambda_g N_g = nf((\sigma_m + \sigma_g)(1 - e^{-\lambda_g t_i}) + (\lambda_g/(\lambda_m - \lambda_g))\sigma_m (e^{-\lambda_m t_i} - e^{-\lambda_g t_i})) \tag{2. 22}$$

For the isomer of Cs^{134}, one can assume $\lambda_g << \lambda_m$ and $e^{-\lambda_g t_i} = 1 - \lambda_g t_i$, then Equation (2. 22) becomes

$$\lambda_g N_g = nf((\sigma_m + \sigma_g)(\lambda_g t_i) + (\lambda_g/\lambda_m)\sigma_m (e^{-\lambda_m t_i} + \lambda_g t_i - 1)) \tag{2. 23}$$

Suppose $A_g^{t_g}$ is the measured absolute activity of Cs^{134g} at time t_g after the end of irradiation, the $A_g^{t_g}$ measured also includes the contribution of the decay of the metastable state to the ground state during the period t_g.

Therefore, the absolute disintegration rate of the ground state at the end of bombardment is given by

$$N_g \lambda_g = \frac{A_g^{t_g}}{e^{-\lambda_g t_g}} - \left(-\frac{\lambda_m^2}{\lambda_g - \lambda_m} N_m e^{-\lambda_m t_g} + \frac{\lambda_m \lambda_g}{\lambda_g - \lambda_m} N_m e^{-\lambda_g t_g}\right) \tag{2. 24}$$

Assuming λ_g is much less than λ_m, Equation (2. 24) can be approximated as

$$N_g\lambda_g \simeq A_g^{t_g} + \lambda_g\lambda_m N_m(e^{-\lambda_m t_g} - e^{-\lambda_g t_g})$$

$$\simeq \frac{A_g^{t_g}}{e^{-\lambda_g t_g}} + \frac{\lambda_g A_m^{t_m} e^{\lambda_m t_m}(e^{-\lambda_m t_g} - 1)}{\lambda_m} \qquad (2.25)$$

Equating (2. 25) and (2. 23), it becomes

$$\frac{A_g^{t_g}}{e^{-\lambda_g t_g}} + \frac{\lambda_g A_m^{t_m} e^{\lambda_m t_m}(e^{-\lambda_m t_g} - 1)}{\lambda_m}$$

$$= nf\{(\sigma_m + \sigma_g)(\lambda_g t_i) + \frac{\lambda_g}{\lambda_m}\sigma_m(e^{-\lambda_m t_i} + \lambda_g t_i - 1\}$$

i. e. ,

$$nf\{(\sigma_m + \sigma_g)(\lambda_g t_i)\}$$

$$= \frac{A_g^{t_g}}{e^{-\lambda_g t_g}} + \frac{\lambda_g A_m^{t_m} e^{\lambda_m t_m}(e^{-\lambda_m t_g} - 1)}{\lambda_m} - \frac{\lambda_g}{\lambda_m}\sigma_m(e^{-\lambda_m t_i} + \lambda_g t_i - 1)nf$$

i. e., $nf\sigma_g(\lambda_g t_i)$

$$= \frac{A_g^{t_g}}{e^{-\lambda_g t_g}} + \frac{\lambda_g A_m^{t_m} e^{\lambda_m t_m}(e^{-\lambda_m t_g} - 1)}{\lambda_m} - \frac{\lambda_g}{\lambda_m}\sigma_m(e^{-\lambda_m t_i} + \lambda_g t_i - 1)$$

$$- nf\sigma_m(\lambda_g t_i)$$

$$\therefore \sigma_g = \frac{A_g^{t_g}}{e^{-\lambda_g t_g}(\lambda_g t_i)nf} + \frac{\lambda_g A_m^{t_m} e^{\lambda_m t_m}(e^{-\lambda_m t_g} - 1)}{\lambda_m nf(\lambda_g t_i)}$$

$$- \frac{\sigma_m}{\lambda_m t_i}(e^{-\lambda_m t_i} + \lambda_g t_i - 1) - \sigma_m$$

$$= \frac{A_g^{t_g}}{e^{-\lambda_g t_g}(\lambda_g t_i)nf} + \frac{A_m^{t_m} e^{\lambda_m t} e^{-\lambda_m t_g}}{\lambda_m t_i nf} - \sigma_m\left[1 + \frac{1}{\lambda_m t_i}(e^{-\lambda_m t_i} + \lambda_g t_i - 1)\right]$$

Since from Equation (2. 6), $\sigma_m = A_m^{t_m} e^{\lambda_m t_m}/(1 - e^{\lambda_m t_i})nf$ then

$$\sigma_g = \frac{A_g^{t_g}}{e^{-\lambda_g t_g}(\lambda_g t_i)nf} + \frac{\sigma_m}{\lambda_m t_i}(1 - e^{-\lambda_m t_i})(e^{-\lambda_m t_g} - 1)$$

(2. 26)

$$- \sigma_m\left[1 + \frac{1}{\lambda_m t_i}(e^{-\lambda_m t_i} + \lambda_g t_i - 1)\right]$$

For the calculation of the ground state isomeric cross-section of Cd^{115}, since the metastable state has a much longer half-life than the ground state, the term $\lambda_m N_m$ from Equation (2. 7) can be neglected. The equation then becomes

$$dN_g/dt = R_g - \lambda_g N_g \qquad (2. 27)$$

The solution of Equation (2. 27) is given by

$$\lambda_g N_g = R_g(1 - e^{-\lambda_g t_i}) \qquad (2.28)$$

Suppose $A_g^{t_g}$ is the absolute disintegration rate at time t_g after the end of irradiation, then $\lambda_g N_g = A_g^{t_g} e^{\lambda_g t_g}$ where $A_g^{t_g}$ is again equal to the rate of net photopeak count divided by the product of the absolute photopeak efficiency of the detector and the branching ratio of the gamma ray measured.

An example for the calculation of Cs^{134} isomeric cross-section ratio for U^{238} (α, f) is shown in Appendix I.

Summary of Experimental Results

The experimental isomeric cross-section ratios for the reactions investigated are summarized in Table 1.

Table 1. Isomer ratios for charged particle induced fission.

Reaction	$U^{238}(\alpha, f)$	$Th^{232}(d, f)$	$Ra^{226}(d, f)$	$Bi^{209}(\alpha,f)$
I. R. of Cd^{115} $(\sigma_m/(\sigma_m+\sigma_g))$	0. 048± 0. 005	0. 063± 0. 010	0. 98±0. 13	0. 9±0.2
I. R. of Cs^{134} $(\sigma_m/(\sigma_m+\sigma_g))$	0. 53± 0. 06	0. 57 ± 0. 05	0. 22±0. 12	

Each reaction was repeated twice except U^{238} fission and the results are the averaged values from two measurements. The uncertainties represent the standard deviation based on counting statistics, decay scheme uncertainties, etc. For the case of $Bi^{209}(\alpha, f)$, the production of Cs^{134} isomers was too low to measure.

A word about the Cd^{115} isomer ratio data seems in order. The Cd^{115} isomer ratios are cumulative yield isomer ratios. Some evidence does exist for cross over transtions in the Ag^{115} - Cd^{115} decay (29) which cause the Ag^{115m} to decay primarily to the Cd^{115g}, thus causing a low value for the Cd^{115} isomer ratio. Thus the measured Cd^{115} isomer ratios represent lower limits on the true "independent-yield" isomer ratios. In the U and Th systems, the independent yields of Cd is not large so that the measured isomer ratio is determined largely by the features of the decay scheme feeding Cd^{115}. For this reason, we choose not to try to analyze the U and Th results further. On the other hand in the Ra^{226} and Bi^{209} systems. Cd is the primary fragment and the values of the isomer ratio are quite large. This means that the contributions of the β-decay precursors to the Cd isomer ratio must be small. Therefore we choose to interpret the value of the Cd^{115} isomer ratio in the fission of Bi^{209} and Ra^{226} as setting a significant lower limit on the fragment angular momentum. The Cs^{134} isomer ratios are independent yield isomer ratios and can be interpreted clearly in terms of the fragment angular momentum.

THEORETICAL CALCULATION OF ISOMER RATIOS

In order to interpret the experimental values of the fragment isomer ratios in terms of the primary fragment angular momentum, further calculations were carried out using the formalism of Vandenbosch and Huizenga (1). Each fragment was assumed to have an initial spin distribution as given by equation (3-4) which was characterized by a root mean square primary fragment angular momentum of $(\bar{J}^2)^{\frac{1}{2}}$. Using the formalism outlined below, the fragment angular momentum distribution after the emission of several neutrons and gamma rays was calculated. From this distribution, the values of the fragment isomer ratios are predicted using gamma ray selection rules. The calculation is done in a trial and error fashion with different values of $(\bar{J}^2)^{\frac{1}{2}}$ being substituted into the calculation until the calculated and experimental values of the isomer ratio agree. The details of the calculation are given in the following sections.

The Mechanism of Nuclear Reaction

In calculating the theoretical isomeric cross-section ratio for a given isotope in nuclear fission, one has to understand the mechanism of the reaction. It is first assumed that the target nucleus absorbs

the incoming projectile to form a compound nucleus C with excitation energy E_c. This nucleus then splits into two fragments A and B with excitation energy E_a and E_b respectively. The deexitation of the fragment occurs mainly by emission of neutrons and by emission of gamma radiation. The process of reaction and fragment deexitation is sketched in Figure 8.

Calculation of Excitation Energies at each Deexcitation Step

The excitation energy of the compound nucleus E_c is equal to the binding energy B_e of the incoming particle plus the kinetic energy of the incoming particle E_I (neglect the recoil energy which is small) i.e.,

$$E_c = B_e + E_I \tag{3.1}$$

When the compound nucleus splits into fragments A and B, the total energy liberated is given by

$$E_d = E_c + (M_c - M_a - M_b) \tag{3.2}$$

where M_c is the mass of the compound nucleus, M_a is the mass of fragment A and M_b is the mass of fragment B.

The total excitation energy of the fragments is given by

$$E_f = E_d - E_{TKE} \tag{3.3}$$

where E_{TKE} is the total kinetic energy of the fragments.

The excitation energy E_f is divided between A and B according to the mass ratio of $(M_a/(M_a + M_b))$, $(M_b/(M_a + M_b))$ respectively. Therefore, the excitation energy of A is $E_f(M_a/(M_a + M_b))$; the excitation of B is $E_f(M_a/(M_a + M_b))$. These divisions of energy corresponds to the assumption of equal temperatures of the two fragments at scission.

The excitation energy of the fragment after emission of a neutron is that left after the subtraction of the neutron binding energy and the kinetic energy carried by the neutron from its original excitation energy. The neutron kinetic energy was assumed to be 2 MeV (36).

For the deexcitation by gamma radiation, it is assumed that on the average, the deexcitation energy is about 1.2 MeV for each step (10).

In the above calculation of excitation energy, the mass formula by Wing and Fong (11) or by Myers and Swiatecki (12) was applied.

Application of Statistical Theory

The total angular momentum of the nucleus can be considered as a vector sum of the spin angular momentum and the orbital angular momentum of the individual protons and neutrons in the nucleus. If the nucleus is in its ground state, the spin of that state can be predicted by the use of the shell model (13). If the nucleus is excited to

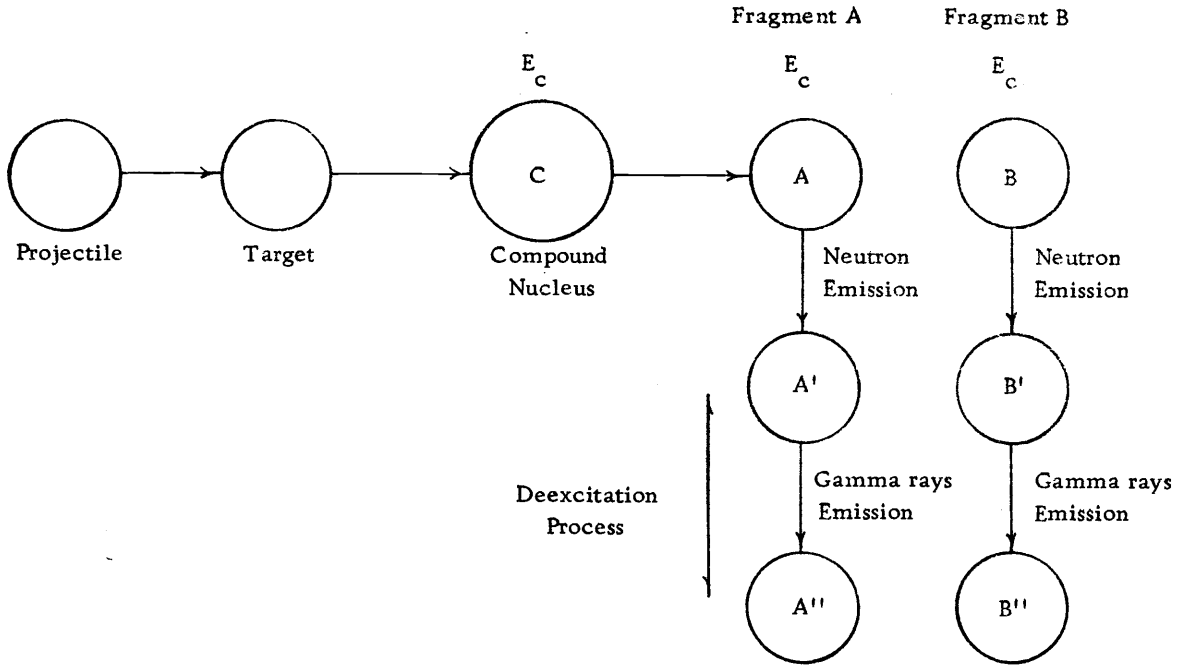

Figure 8. Deexcitation process of fission fragments.

more than a few MeV, there are many levels available, therefore the application of statistical model (14-16) is valid. In statistical theory, one speaks of level densities which is the number of levels per MeV. The level density increases exponentially with the excitation energy of the nucleus. In this case, one is concerned with the spin distribution of levels within a small energy interval. At a given excitation energy E, the level density having an angular momentum J is given by (17-18) $\rho(J) = \rho(0)(2J + 1)e^{-(J + \frac{1}{2})^2/2\sigma^2}$ where $\rho(0)$ is the density of levels having angular momentum o, σ is a parameter called the spin cut-off factor.

Calculation of the Angular Momentum Distribution of the Primary Fragment

In calculating the average spin of the primary fragment, one assumes a functional form for the fragment spin distribution of form

$$N(J) = (2J + 1) \exp. (-J(J + 1)/2b^2) \qquad (3.4)$$

where b is a parameter. This distribution has a mean square angular momentum value of $J^2 = 2b^2$. It is the same form of fragment spin distribution predicted by Nix and Swiatecki (34). Therefore, it one assumes an average

initial angular momentum J for the fragment, the angular momentum distribution of the primary fragment can be calculated by using formula (3.4). (Detailed calculations have shown that the results of our calculations are independent of the form of the initial spin distribution as long as reasonable distributions (Gaussian, "picket fence" etc.) are chosen.)

Sample calculations for the normalized distribution of J for average J equal to 4, 10 and 15 are shown in Tables 2, 3 and 4.

A plot of the distribution of J versus J, i.e., $N(J)$ versus J is shown in Figure 9 for average J equal to 4, 10 and 15.

Calculation of the Angular Momentum of the Fragment after Neutron Emission

According to Hafner et al. (20), the primary fragment in a particular state having angular momentum J_c can decay by neutron emission to final states with different spin values, each of which are denoted by J_f. The relative probability for a state J_c decaying by emitting a neutron to a final state J_f is given by (20)

$$P(J_f)_{J_c} \propto \rho(J_f) \sum_{s=|J_f-s'|}^{J_f+s'} \sum_{\ell'=|J_c-s|}^{J_c+s} T_{\ell'}(E)$$

where s' is the intrinsic spin of neutron ($s'=\frac{1}{2}$), $T_\ell(E)$ is the neutron transmission coefficient with angular momentum ℓ and energy E and

Table 2. Normalized spin distribution for $J = 4$.

J	$J(J+1)$	$\frac{-J(J+1)}{2b^2}$	e^{-A}	$(2J+1)$	N(J)	$A = \frac{-J(J+1)}{2b^2}$ N(J) (Normalized)
	$<\sqrt{J}^2> = 4$			$2b^2 = 16$		
0	0	0	1	1	1	0.06120
1	2	0.125	0.884	3	2.649	0.16274
2	6	0.375	0.687	5	3.425	0.20967
3	12	0.750	0.471	7	3.297	0.20483
4	20	1.25	0.286	9	2.574	0.15757
5	30	1.87	0.154	11	1.694	0.10376
6	42	2.62	0.074	13	0.962	0.05889
7	56	3.50	0.030	15	0.450	0.02754
8	72	4.50	0.011	17	0.187	0.01144
9	90	5.62	0.004	19	0.076	0.00465
10	110	6.87	0.001	21	0.021	0.00135
					$\sum = 16.335$	

Table 3. Normalized spin distribution for J = 10.

J	$\langle\sqrt{J^2}\rangle = 10$ J(J+1)	$-\frac{J(J+1)}{2b^2}$	e^{-A}	$10^2 = 2b^2 = 100$ (2J+1)	N(J)	$A = \frac{-J(J+1)}{2b^2}$ N(J)
0	0	0	1	1	1	0.01003
1	2	0.020	0.980	3	2.940	0.02951
2	6	0.060	0.942	5	4.710	0.04728
3	12	0.120	0.887	7	6.209	0.06233
4	20	0.200	0.817	9	7.353	0.07381
5	30	0.300	0.740	11	8.140	0.08171
6	42	0.420	0.656	13	8.528	0.08561
7	56	0.560	0.571	15	8.565	0.08598
8	92	0.720	0.486	17	8.262	0.08294
9	90	0.900	0.406	19	7.714	0.07744
10	110	1.000	0.367	21	7.707	0.07737
11	132	1.32	0.267	23	6.141	0.06164
12	156	1.56	0.210	25	5.250	0.05270
13	182	1.82	0.162	27	4.374	0.04391
14	210	2.10	0.122	29	3.538	0.03551
15	240	2.40	0.090	31	2.700	0.02710
16	272	2.72	0.066	33	2.178	0.02186
17	306	3.06	0.047	35	1.645	0.01651
18	342	3.42	0.032	37	1.184	0.01188
19	380	3.80	0.022	39	0.858	0.00861
20	420	4.20	0.015	41	0.615	0.00627
					$\sum = 99.611$	

Table 4. Normalized spin distribution for J = 15.

J	J(J+1)	$-\frac{J(J+1)}{2b^2}$	e^{-A}	2J+1	N(J)	N(J) (Normalized)
	$<\sqrt{J^2}> = 15$			$2b^2 = 225$		$A = \frac{-J(J+1)}{2b^2}$
0	0	0	1	1	1	0.00518
1	2	0.009	0.990	3	2.970	0.01539
2	6	0.027	0.973	5	4.865	0.02521
3	12	0.053	0.948	7	6.636	0.03439
4	20	0.089	0.915	9	8.235	0.04267
5	30	0.133	0.876	11	9.636	0.04994
6	42	0.187	0.830	13	10.790	0.05592
7	56	0.249	0.780	15	11.700	0.06064
8	72	0.320	0.726	17	12.342	0.06396
9	90	0.400	0.670	19	12.730	0.06597
10	110	0.489	0.614	21	12.894	0.06682
11	132	0.587	0.556	23	13.788	0.06628
12	156	0.693	0.500	25	12.500	0.06478
13	182	0.809	0.446	27	12.042	0.06240
14	210	0.933	0.394	29	11.426	0.05921
15	240	1.067	0.322	31	9.982	0.05173
16	272	1.210	0.298	33	9.834	0.05096
17	306	1.360	0.257	35	8.995	0.04661
18	342	1.520	0.219	37	8.103	0.04199
19	380	1.689	0.186	39	7.254	0.03759
20	420	1.867	0.152	41	6.232	0.03236
					$\sum = 192.95$	

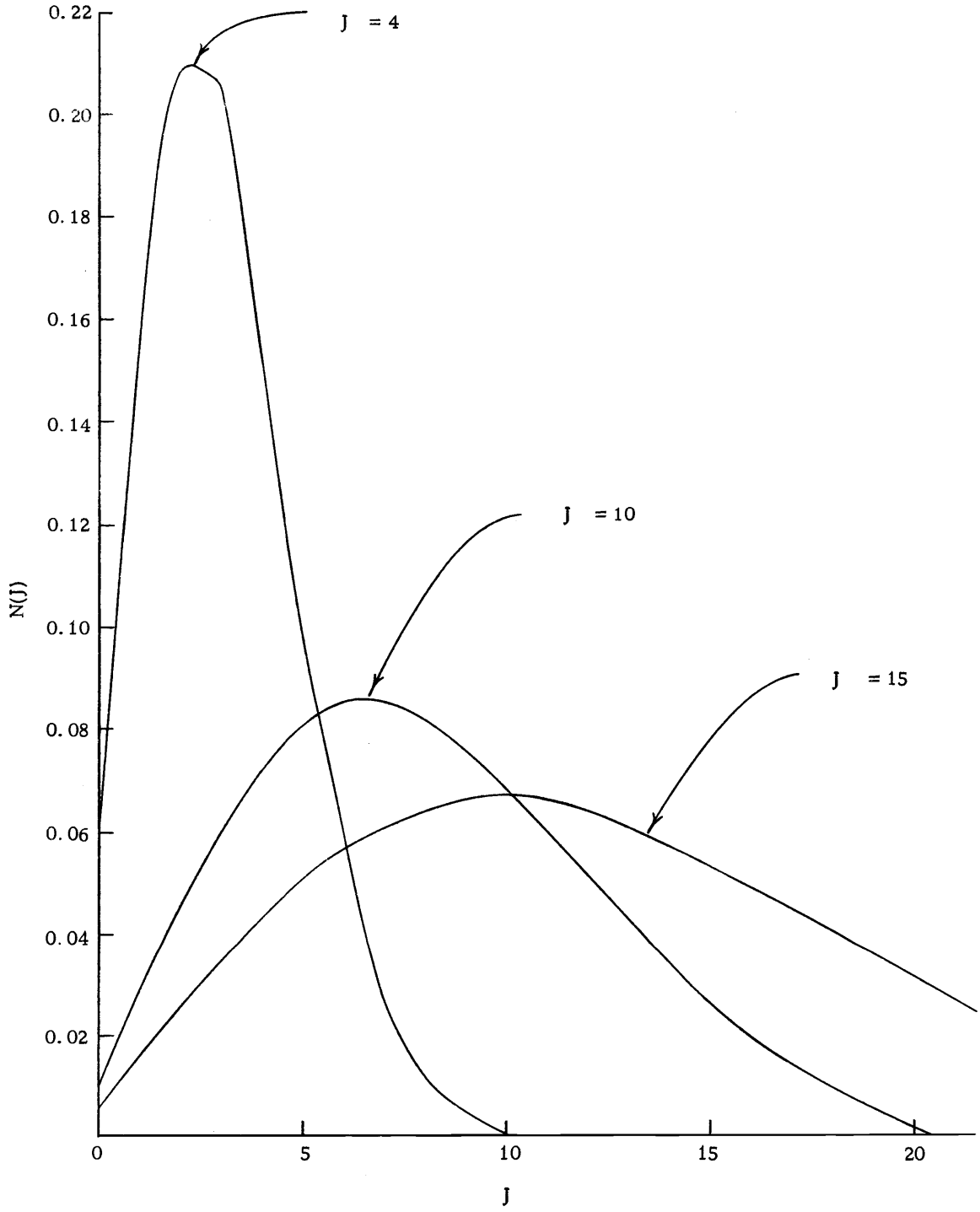

Figure 9. Plot of N(J) v. J .

$$\rho(J_f) \propto (2J_f+1)\exp\left[-(J_f+\tfrac{1}{2})^2/2\sigma^2\right]$$

Since this is only concerned with the relative probability, the yield of spin J_f has to be normalized by multiplying the initial normalized yield of J_c by the fraction of J_c decaying to J_f. **Therefore, the** total normalized field of J_f is calculated by adding over all values of J_c and is given by

$$P_{J_f} = \sum_{J_c=\begin{cases} J_{c_I} \text{ for } (J_f - \ell_{max} - s') \leq 0 \\ J_f - \ell_{max} - s' \text{ for } (J_f - \ell_{max} - s') > 0 \end{cases}}^{\begin{cases} J_{c_{max}} \text{ for } (J_f + \ell'_{max} + s') \geq J_{c_{max}} \\ J_f + \ell_{max} + s' \text{ for } (J_f + \ell'_{max} + s') < J_{c_{max}} \end{cases}} P_{J_c} \times$$

$$\frac{\rho_{J_F} \sum_{s=|J_f - s'|}^{J_f+s'} \sum_{\ell'=|J_c - s|}^{J_c+s} T'_{\ell'}}{\sum_{J_f=J_c+\ell'_{max}+s'}^{J_f=\begin{cases} J_{f_I} \text{ for } (J_c - \ell_{max} - s') \leq 0 \\ J_c - \ell'_{max} - s' \text{ for } (J_c - \ell'_{max} - s') > 0 \end{cases}} \rho_{J_f} \sum_{s=|J_f - s'|}^{J_f+s'} \sum_{\ell'=|J_c - s|}^{J_c+s} T'_{\ell'}}$$

where $J_{f_{max}} = \ell'_{max} + s' + J_{c_{max}}$

$J_{c_{max}}$ = maximum value of the index J_c from the input P_{J_c}

$$\rho_{J_f} = (2J_f + 1) \exp \frac{-(J_f + \frac{1}{2})^2}{2\sigma^2} \quad \text{for } J_f = J_{f_I},\ J_{f_I}+1, \cdots J_{f_{max}}$$

J_{c_I}, J_{f_I} are initial values of the indices J_c and J_f.

P_{J_c} are the normalized initial spin distribution from the initial compound nucleus.

$T'_{\ell'}$ are the transmission coefficients

s' is the outgoing particle spin

ℓ'_{max} is the maximum value of the index ℓ' for the input $T_{\ell'}$.

Calculation of the Spin Distribution of Fragment after Emission of Gamma Radiation

According to statistical theory, it is assumed that the primary fragment after emitting neutrons will emit gamma rays for the final stage of deexcitation. According to Hafner et al. (20), the probability of decaying from state J_i to state of J_f is assumed to be proportional to the density of final states with spin J_f. Once again, the total distribution has to be normalized. Therefore, the normalized yield of J_f is given by

$$F_{J_f} = \sum_{J_i = |J_f - \ell|}^{J_f + \ell} F_{J_i}\, \rho(J_f)\, \delta_{J_i, J_f} \Big/ \sum_{J_f = |J_i - \ell|}^{J_i + \ell} \rho(J_f)$$

where $\rho(J_f) = (2J_f + 1) \exp - (J_f + \frac{1}{2})^2 / 2\sigma^2$

ℓ is the multipolarity of gamma emission

σ is the spin cut-off factor

F_{J_i} is the normalized initial spin distribution (following last particle emission)

$$J_{f_{max}} = J_{i_{max}} + \ell \quad \text{and} \quad \delta_{J_i, J_f} = 1 \quad \text{if} \quad |J_i - J_f| \leq \ell \leq |J_i + J_f|$$

$$\delta_{J_i, J_f} = 0 \,[1]$$

It is assumed that the excited nucleus just prior to the last gamma deexcitation chooses to feed the metastable or ground state depending on which transition has the smaller spin change. The theoretical isomeric ratio defined as $\sigma_m/(\sigma_m + \sigma_g)$ is then the sum of the normalized probability of the corresponding spins that will populate the metastable state. For example, if the metastable state has spin 2 and the ground state has spin 5, then the states having spin 0, 1, 2 and 3 will populate the spin 2 state, and states with spin 4 or greater will populate the spin 5 state. Then the isomeric cross-section ratio $\sigma_m/(\sigma_m + \sigma_g)$ will be the sum of the normalized probability of spin 0, 1, 2 and 3.

In summary, what was done to interpret the experimental isomer ratio values was to substitute a value of the initial primary

---

[1] This condition is due to the selection rule forbidding proton transition such as 0→0 for dipole and 0→0, 0→1, and 1→0 for quadrupole.

fragment angular momentum $(\bar{J}^2)^{\frac{1}{2}}$, into equation (3-4), carry out the calculation of the neutron and γ-ray cascade using the formalism outlined above, until a value of the isomer ratio was obtained. Then the value of the isomer ratio agrees with the experimental value thus allowing deduction of the average initial fragment angular momentum.

The Assumption Involved in the Calculation of Isomer Ratios and Their Validity

The theoretical calculation of the isomeric cross-section ratio as outlined in this chapter involves the assignment of an average initial angular momentum to the primary fragment, the calculation of the deexcitation process energetics and finally the calculation of the spin distribution following each deexcitation step. The process terminates when the γ-ray cascade populates either the metastable or ground state of the product nucleus thus leading to a theoretical estimate of the isomer ratio.

The largest uncertainty in the calculation involves the specification of the energetics of the deexcitation process. The unknown quantity is the total excitation energy of each fragment. This affects the number of neutrons and γ-rays emitted in the deexcitation cascade and most importantly, the values of the spin cut-off parameters, $\sigma(E)$, used to characterize the angular momentum dependence of the level density of the fragments during the deexcitation process. In this work a modern mass formula (11) and measured fragment total kinetic energies (21, 22) were used to calculate the energy available for dissipation in the neutron-γ-ray cascade. It was further assumed that the spin cut-off parameter, σ, could be calculated using rigid body

values of the fragment moment of inertia, i.e.,

$$\sigma^2 = \frac{It}{\hbar^2}$$

where I is the rigid body moment of inertia of the fragment based on a nuclear radius parameter of 1.2×10^{-13} cm. and t is the nuclear temperature which is defined (23) by the relationship $E = at^2 - t$. Here E is the fragment excitation energy and a, the level density parameter, was set equal to A/8 (MeV^{-1}) where A is the mass number of the fragment.

It is known that there are certain difficulties connected with this approach. The energy balance calculations of Schmitt and co-workers (24) have shown that the predictions of the fragment excitation energy using the method outlined above may be in error by as much as 10 MeV. The seriousness of this discrepancy is pointed out by calculations that show that a change of the value of σ by ± 0.5 in the last stages of the neutron-γ ray cascade will change the isomeric cross-section ratio by $\pm 10\%$. Furthermore, there is ample theoretical and experimental evidence (see, for example, the review article of Thomas (25)) that the effective fragment moment of inertia is reduced below the rigid body value at low excitation energy.

However, Loveland (26) has examined this question in detail. He has used proper superconductor model calculations of the excitation energy dependence of the moment of inertia and a range of empirical and mass-formula based calculations of the energetics of the deexcitation

process. His results show that although the absolute magnitude of the fragment angular momentum is somewhat uncertain due to uncertainties in the energetics calculations, the qualitative trend of the J values deduced for the various fissioning systems is well reproduced by the calculational procedure described above. Loveland's results, although not a part of this work are listed in Table 5 for comparison with the calculations of this work.

The multipolarity of the γ radiation was assumed to be dipole even though there is evidence (27, 28) that the γ-radiation following fission is primarily quadrupole. This assumption of dipole radiation was made so as to keep the calculation parameters similar to those used by other investigators (30) who have studied isomer ratios in nuclear reactions where the initial angular momentum distribution was well known. Furthermore calculations show that the isomeric cross-section ratio is quite insensitive to the decay mode. (The isomer ratio of Cs^{134} in U^{238} (α, f) changes by 5% if one assumes quadrupole instead of dipole radiation.)

Sample Calculation of Isomer Ratio

A sample calculation is shown here for the case of the Cs^{134} isomer ratio in the Th^{232} (20 MeV d, f) reaction. The actual calculations were made using the computer program of Hafner et al. (20).

(The program listings and sample output are shown in Appendix II.)

The reaction energetics are shown in Figure 10.

In Figure 10, it is shown that a Th^{232} nucleus being bombarded by 20 MeV deuterons, thus forming the compound nucleus Pa^{234} at an excitation energy of 27.9 MeV. The Pa^{234} fissions and one of the fragments is Cs^{136} which deexcites by emitting two neutrons and three statistical γ-rays followed by a final γ-ray transition to populate either the metastable or ground state of Cs^{134}. The fragment excitation energies and spin cut-off parameters are shown at each step.

The normalized spin distribution values after the emission of the third "statistical" γ-ray are shown in Appendix II and Table 5.

Table 5. Final normalized spin distribution values for Cs^{134} fragment in Th^{232} (20 MeV d, f) reaction. ($\sqrt{\bar{J}^2}$ assumed to be 11 $\hbar$)

J	P(J)	J	P(J)
0	0.001846	11	0.062802
1	0.015458	12	0.052410
2	0.037365	13	0.042526
3	0.060271	14	0.033584
4	0.078635	15	0.025834
5	0.090173	16	0.019370
6	0.095077	17	0.014165
7	0.094561	18	0.010108
8	0.089955	19	0.007040
9	0.082443	20	0.004789
10	0.073079	21	0.003183

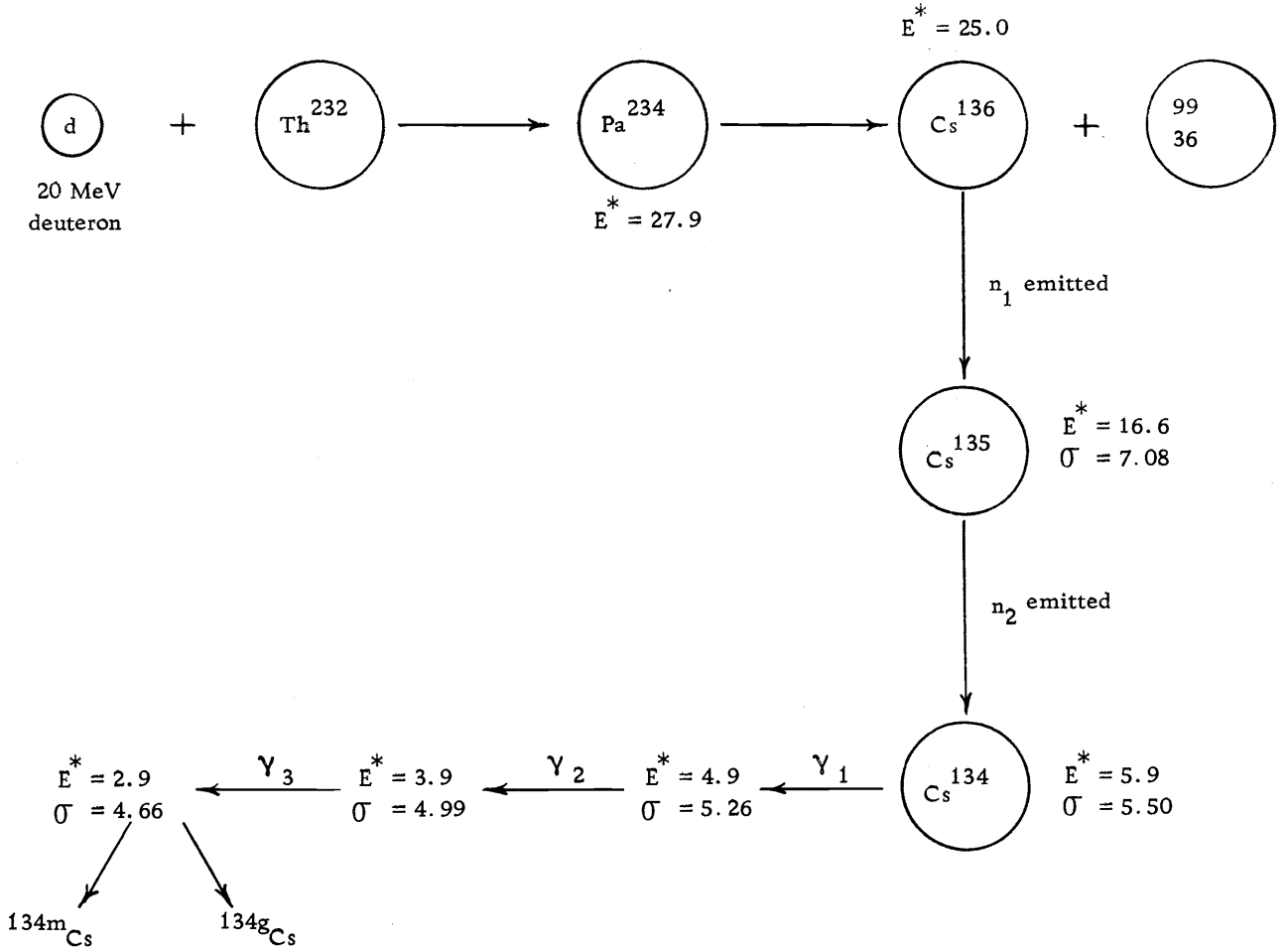

Figure 10. The reaction process of Th^{232} (d, f).

Using the decay scheme shown in Figure 6 as a basis we assume that all members of the spin population distribution with $J \leq 6$ will decay to the 4+ ground state (via the low-lying 5+ level at 10 keV) while those members with $J > 6$ will populate the 8+ metastable state. Thus the theoretical isomer ratio $(\sigma_m/(\sigma_m + \sigma_g))$ is 0.62 for $\sqrt{\overline{J^2}} = 11\hbar$.

This calculation neglects the contributions of second or greater chance fission, but calculations of the Cs^{134} isomer ratio including the effects of multiple chance fission do not differ from those outlined above by more than $1\hbar$.

Summary of Calculations

A summary of the results of the calculations is shown in Table 6.

Table 6. Fission fragment angular momentum for charged particle induced fission calculated from experimental values of isomer ratios.

Fission Reaction	Fragment Studied	$(\overline{J^2})^{\frac{1}{2}}$ ($\hbar$)	
		Rigid Body Moment	Superconductor Moment (26)
U^{238} (35 MeV α, f)	Cs^{134}	9 ± 1	11 ± 1
Th^{232} (20 MeV d, f)	Cs^{134}	11 ± 1	13 ± 1
Ra^{226} (19 MeV d, f)	Cs^{134}	5 ± 2	7 ± 2
	Cd^{115}	>14 ± 3	>15 ± 4
Bi^{209} (35 MeV α, f)	Cd^{115}	> 9 ± 4	>13 ± 4

CONCLUSIONS AND DISCUSSION

From the average initial fragment angular momenta shown in Table 6, one can conclude:

1. Although the absolute magnitudes of the fragment angular momenta are somewhat uncertain due to the uncertainty in our knowledge of the deexcitation cascade, one can say, in general, that the fragment angular momenta in charged particle induced fission are greater than those in low energy induced fission. (J values for low energy and spontaneous fission range from 4 - 8 $\hbar$ (31)).

2. There seems to be no correlation between the angular momentum of the initial compound nucleus in fission and the fragment angular momentum. For example, in the Pa^{234} and Pu^{242} fissioning systems, the compound nuclear angular momenta are 8 $\hbar$ and 13 $\hbar$, respectively. Yet in these same systems, the fragment angular momenta are 13 $\hbar$ and 11 $\hbar$, respectively, for Pa^{234} and Pu^{242}.

3. The results, along with the measurement of Loveland and Hill (32) who found that J = 15 $\hbar$ for the Nb^{95} fragment in Bi^{209} (35 MeV α, f), seem to indicate a trend for the fragment angular momentum to increase as the (Z, A) of the fissioning system decrease.

What effect do these experimental findings have upon our understanding of the dynamics of the scission stage of the fission process? In order to answer this question, it will be necessary to briefly outline some of the theoretical models for the "generation" of fragment angular momentum in fission. It has been suggested that there are two principal components to the fragment angular momentum in fission. They are:

1. A post-scission electrostatic torque due to non-axial breaking of the neck between the two nascent fragments at scission. The situation is illustrated in Figure 11a. A torque is generated on each fragment due to the Coulomb repulsion between the fragment stub and the fragment. In a simple rigid body dynamical estimate, Rasmussen et al. (35) showed that the fragment angular momentum due to this sort of effect might be given by

$$\Delta\ell_B = (\tfrac{1}{2} e^2 M_r Z_A)^{\frac{1}{2}} \frac{Q_B \gamma_0}{\sigma_c^{3/2}}$$

where M_r is the system reduced mass, Z_A the charge of fragment A, Q_B the quadrupole moment of fragment B, σ_c the fragment center to center distance and γ_0 is the angle between the symmetry axis of the deformed fragment and the center to center vector.

2. A prescission excitation of the rotational levels of the fragments. This approach was suggested by Nix and Swiatcki in a

semi-classical model (34) and Rasmussen et al. (35) in a quantum mechanical approach. The latter authors have asserted that due to the deformed fragments interacting in a strong Coulomb field that there will be a "zero-point" excitation of rotational levels in the fragments thus giving rise to fragment angular momentum. Rasmussen et al. calculate a $J \tilde{=} 5 - 6\hbar$ for the Ru^{108} fragment in Pu^{239} (n, f) due to their mechanism. They assert that the average fragment angular momentum due to this effect can be given by the equation

$$\ell + \tfrac{1}{2} = \frac{\sqrt{\pi}}{2\gamma_0}$$

where γ_0 is the angle between the summetry axis of the deformed fragment and the center to center vector. The functional dependence of γ_0 is given as

$$\gamma_0 = \frac{\hbar^{\frac{1}{2}}}{(KB)^{\frac{1}{4}}}$$

where B is the initial parameter for bending motion and K depends directly on the fragment deformation and inversely on the fragment separation. The point is that ℓ depends only on the fourth root of the fragment deformation and inversely as the fourth root of the fragment separation.

Thus it would seem that the two theoretical models proposed to account for the fragment angular momentum have rather differing

predictions of the dependence of J upon parameters such as fragment deformation and separation. Before proceeding further, however, with this discussion, a note of caution must be sounded. The proponents of these two models have not attempted to make predictions of J for the fissioning systems studied. Perhaps when and if they do so, other effects will be discovered which have been neglected in their treatments up to this point. The remarks which follow should only be regarded as a speculative rather than definitive attempt to confront theory and experiment.

Nonetheless it would appear that the sharp changes in J with the excitation energy of the fissioning system and the (Z, A) of the fissioning system would be very difficult to explain in the framework of a model like that attributing a major fraction of the fragment angular momentum to prescission excitation of fragment rotational bands. The theory simply predicts J to be rather insensitive to changes of the type we have studied.

Whether or not our results can be accounted for in the framework of the "post-scission electrostatic torque" model remains an open question. Too little knowledge of the scission point parameters such as fragment deformation and separation is available to permit a definitive test. However a simplistic and speculative model does exist that will qualitatively account for our results.

To explain the increase in J in going from Pu^{242} to At^{213} in the face of decreasing fragment Z and slightly increasing σ_c one notes that the fragments may become much more deformed leading to greater increased Coulomb interaction and subsequent angular momentum (see Figure 11b). Furthermore, the increase in J with system excitation energy may also be due to increased fragment deformation with little change in σ_c (see Figure 11c). This simplistic model is very similar to Loveland's "zero-order" model (31) which correctly predicted the trend of J with mass-asymmetry in Cf^{252} spontaneous fission.

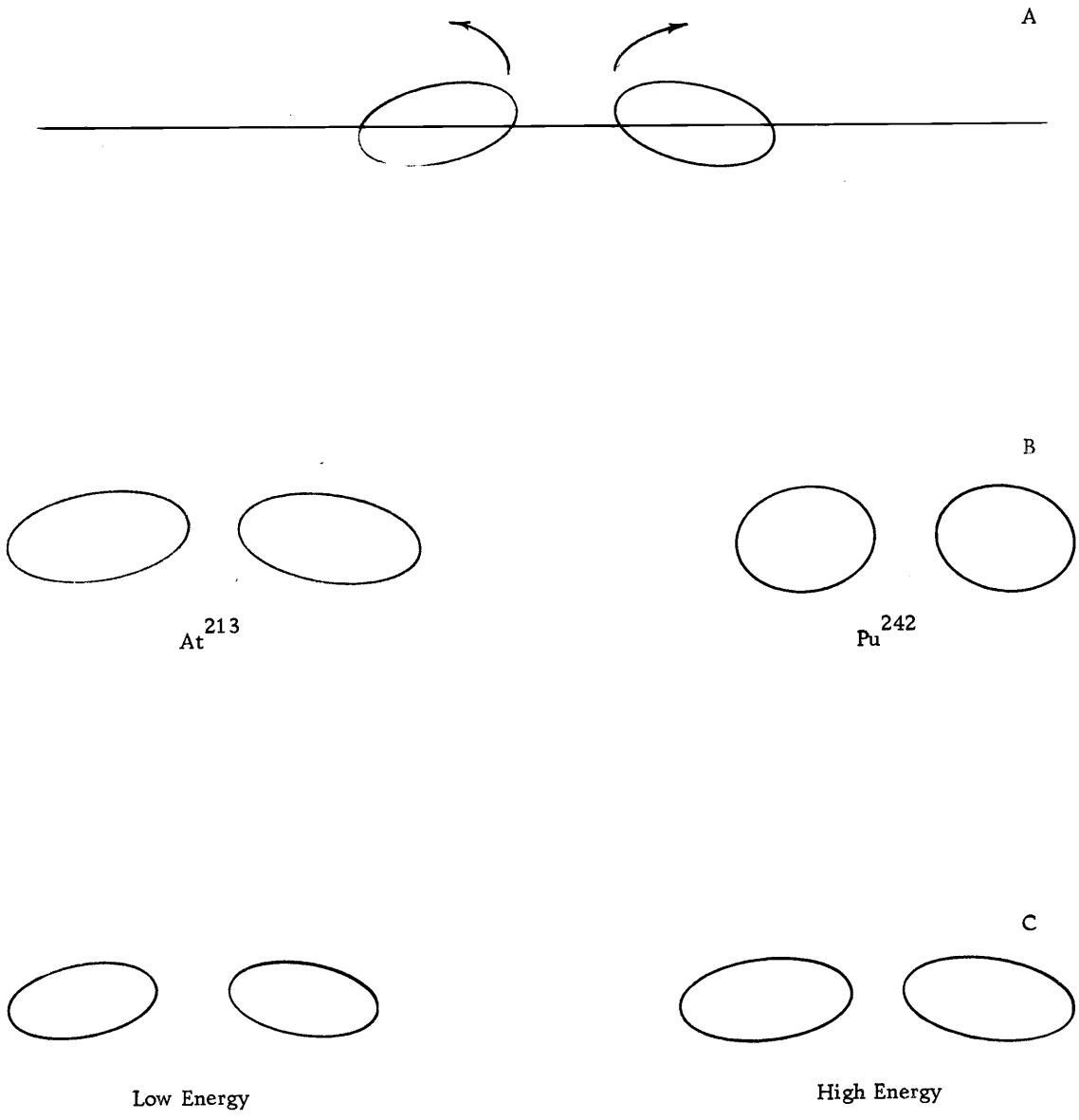

Figure 11. Splitting of fission fragments.

BIBLIOGRAPHY

1. Huizenga, J. R. and R. Vandenbosch, Phys. Rev. 120, 1305 (1960).

2. Glover, K. M. and P. Borrell, J. Nucl. Energy 1, 214 (1955).

3. DeVoe, J. R. and W. W. Meinke, Anal. Chem. 31, 1428 (1959).

4. Glendenin, L. E. and C. M. Nelson. Perchlorate Method for the Determination of Cesium Activity in Fission, in Radiochemical Studies: The Fission Products, C. D. Coryell and N. Sugarman, Eds. National Nuclear Energy Series, Division IV, Vol. 9 (McGraw-Hill, New York, 1951), p. 1642.

5. Freck, D. V. and J. Wakefield, Nature 193, 669 (1962).

6. Webb, P. P. and R. L. Williams, Nucl. Instr. and Meth. 22, 361 (1963).

7. Tavendale, A. J. and G. T. Ewan, Nucl. Instr. and Method. 25, 185 (1963).

8. Lederer, C. M., J. M. Hollander and I. Perlman, Table of Isotopes, Sixth Edition (Wiley, New York, 1967).

9. Chu, Y. L., Charged Particle-Induced Fission: A Mass-Spectrometric Yield Study, UCRL-8926, November, 1959.

10. Johansson, S. A. E. and P. D. Kleinheinz, Gamma Rays in Nuclear Fission in α, β and γ-Spectroscopy, K. Seigbahn, Ed., Vol. 1. (North-Holland, Amsterdam, 1966), p. 805.

11. Wing, J. and J. D. Varley, Calculated Values of Wing-Fong's Nuclidic Mass Equation, ANL-6886, May, 1964.

12. Myers, W. D. and W. J. Swiatecki, Nuclear Masses and Deformations, UCRL 11980, May, 1965.

13. Mayer, M. G., Phys. Rev. 74, 235 (1948); 76, 1622 (1956).

14. Ericson, T., Adv. Phys. 9, 425 (1960).

15. Blatt, J. M. and V. F. Weisskopf, Theoretical Nuclear Physics (Wiley, New York, 1952).

16. LeCouteur, K. J., Statistical Theory in Nuclear Reactions, Vol. 1, (Interscience, New York, 1959), p. 348.

17. Bethe, H. A., Rev. Mod. Phys. 9, 84 (1937).

18. Bloch, C., Phys. Rev. 93, 1094 (1954).

19. Warhanek, H. and R. Vandenbosch, J. Inorg. Nucl. Chem. 26, 669 (1964).

20. Hafner, W. L., J. R. Huizenga and R. Vandenbosch, Computer Program for Calculating the Relative Yields of Isomers Produced in Nuclear Reactions, ANL-6662, December, 1962.

21. Unik, J. P. and J. R. Huizenga, Phys. Rev. 134, B90 (1964).

22. Britt, H. C., H. E. Wegner and J. Gursky, Phys. Rev. 129, 2239 (1963).

23. LeCouteur, K. J. and D. W. Lang, Nucl. Phys. 13, 32 (1959).

24. Plasil, F., R. L. Ferguson and H. W. Schmitt, Neutron Emission in the Fission of ^{215}At in Physics and Chemistry of Fission, (AEA, Vienna, 1969), p. 505.

25. Thomas, T. D., Ann. Rev. Nucl. Sci. 18, 343 (1968).

26. Loveland, W., private communication.

27. Hoffman, M., Phys. Rev. 133, 5714 (1964).

28. Blinov, M. V., N. M. Kazarinov, A. N. Protopopov and B. M. Shiryaw, Sov. Phys. JETP 16, 1159 (1963).

29. Kielberg, A., A. C. Pappas and T. Tunaal, J. Energ. Nucl. Chem. 30, 337 (1968)

30. Dudey, N. D. and T. T. Sugihara, Phys. Rev. 139, 8896 (1965).

31. Loveland, W., Bull. Am. Phys. Soc. 15, 647 (1970).

32. Loveland, W. and D. W. Hill, private communication.

33. Strutinski, V. M., Sov. Phys. JETP 10, 613 (1961).

34. Nix, J. R. and W. J. Swiatecki, Nucl. Phys. 71, 1 (1964).

35. Rasmussen, J. D., W. Nörenberg and H. J. Mang, Nucl. Phys. A136, 465 (1969).

36. J. Gindler and J. R. Huizenga. "Nuclear Fission" in Nuclear Chemistry, Vol. II, L. Yaffee, Ed. (Prentice Hall, 1969)

APPENDICES

APPENDIX I

Sample Calculation of Experimental Isomer Ratio of Cs^{134} in U^{238} (α, f)

After radiochemical separation of Cs , the sample was counted immediately.

For Cs^{134m}, ($t_{\frac{1}{2}}$ = 2.91 hours), the peak at 0.128 MeV was integrated and the net counts were plotted as a function of time until its half-life was identified. The counting results were as follows:

Count No.	Total Counts (40 min.)	Background (40 min.)	Net Count (40 min.)	Time after E. O. B.
1	124267	103258	21009	202 min.
2	68022	50609	17413	253 min.
3	44775	29920	14850	309 min.
4	34466	23001	11465	370 min.
5	29711	20230	9481	423 min.
6	26839	19023	7816	519 min.
7	24678	18292	6386	595 min.

A plot of the net count rate in logarithmic unit vs. time showed a straight line with $t_{\frac{1}{2}} \cong$ 2.95 hours.

One can pick a point on the straight line and calculate its activity at the end of bombardment.

Suppose count #3 was chosen, therefore, the net count rate at the end of bombardment was given by

$$A = \frac{(44775 - 29920)}{40 \text{ min.}} \times \exp.(0.693 \times 309/174.6) + \frac{(44775)}{40} e^{\frac{0.693}{174.6} \times 309}$$

$$= 1.187 \times 10^{3} \pm 17 \text{ c. p. m.}$$

$$= (1.187 \times 10^{3} \pm 1.2\%) \text{ c. p. m.}$$

Assuming absolute photopeak efficiency of detector was equal to $1.42 \times 10^{-3} \pm 5\%$, and the branching ratio of photopeak $14\% \pm 0.5\%$, then the absolute activity of the metastable state at the end of bombardment was given by

$$\mathring{A}_m = \frac{1.187 \times 10^{3}}{1.42 \times 10^{-3}} \times \frac{100}{14} \pm (0.05^2 + 0.012^2 + 0.005^2)^{\frac{1}{2}}$$

$$= (5.97 \times 10^{6} \pm 5.5\%) \text{ d. p. m.}$$

The time of bombardment $t_b = 1.81$ hours. The cross-section for the formation of the metastable state was

$$\sigma_m = 5.97 \times 10^{6}/(1 - e^{-\lambda_m t_b}) n\phi \pm 5.5\%$$

$$= 1.71 \times 10^{7}/n\phi \pm 5.5\%$$

For the Cs^{134g}, the 0.796 and 0.808 MeV peaks were measured twice. First measurement was at 35 days after the end of bombardment and the second measurement was at 97 days after the end of bombardment. The results obtained for both measurements were about the same. Considering the second measurement, the total count rate

was given by 196855/5805 c. p. m. After background subtraction, the net count rate was equal to

$$A = 66839/5805 + (196855)^{\frac{1}{2}}/5805 = (11.5 \pm 6.6\%) \text{ c. p. m.}$$

Assuming the absolute efficiency of the detector was $1.03 \text{ s } 10^{-2} \pm 5\%$ and the branching ratio for the gamma rays 99% ± 0.5%, the absolute disintegration rate at the end of bombardment was

$$\overset{\circ}{A}_g = \frac{11.5 \times 100}{1.03 \times 10^{-2} \times 99} \times e^{\frac{0.693}{2.65} \times \frac{3.56}{12}} \pm 8.2\%$$

$$= (1.23 \times 10^3 \pm 8.2\%) \text{ d. p. m.}$$

According to 3-26, the cross-section for the formation of the ground state was given by

$$\sigma_g = \frac{1.49 \times 10^7}{n\phi} \pm 10\%$$

Therefore, the isomeric cross-section ratio was given by

$$\text{I. R.} = \frac{\sigma_m}{\sigma_m + \sigma_g} = 0.534 \pm 12\%$$

$$= 0.534 \pm 0.064$$

APPENDIX II

Computer Program Listing with Sample Output

PROGRAM LISTING

```
C       NORMALIZED  SPIN  DISTRIBUTIONS  IN  NUCLEAR  REACTIONS
        DIMENSION TL(200),PJC(200),PJF(200),CS(200)
       2 , RHO(200),FJI(200),FJFS(200)
        EQUIVALENCE (RHO,TL),(FJI,PJF),(PJC,FJFS)
 1001   DO 101 I=1,200
        TL(I)=0.0
        CS(I)=0.
        PJF(I)=0.
        RHO(I)=0.
        FJI(I)=0.
        FJFS(I)=0.
  101   PJC(I)=0.0
22222   KTAPE=6
  100   READ 109
  109   FORMAT(72H
       1                    )
         READ 99,MPD
        GO TO(1100,1000,9001,1100,1000,1100),MPD
C
C       NORMALIZED  SPIN  DISTRIBUTION  FOR  INITIAL  COMPOUND  NUCLEUS
C
 1100   READ 1, TSPIN,PSPIN,PORPC,NTL
    1   FORMAT (3E15.8, I3)
        DO 33 I=1,NTL
   33   READ 990,TL(I),CL
        WRITE OUTPUT TAPE KTAPE,1111
 1111   FORMAT(1H1,15X,58HNORMALIZED  INITIAL  COMPOUND  NUCLEUS  SPIN  DI
       1STRIBUTION,/ /)
        WRITE OUTPUT TAPE KTAPE, 109
        WRITE OUTPUT TAPE KTAPE, 200,TSPIN
  200   FORMAT(1H0,10X,22HINPUT TARGET SPIN WAS F6.3)
        WRITE OUTPUT TAPE KTAPE, 201,PSPIN
  201   FORMAT(1H0,10X,26HINPUT PROJECTILE SPIN WAS F6.3)
        WRITE OUTPUT TAPE KTAPE, 202,PORPC
  202   FORMAT(1H0,10X,29HPROPORTIONALITY CONSTANT WAS F6.3)
        FJMAX=TSPIN+PSPIN+CL
        WRITE OUTPUT TAPE KTAPE, 112,FJMAX
  112   FORMAT(1H0,10X,39HJCMAX=LMAX+TARGET SPIN+PROJECTILE SPIN=F4.1)
        C=(2.*PSPIN+1.)*(2.*TSPIN+1.)
        SUL=ABSF(TSPIN+PSPIN)
        SLL=ABSF(TSPIN-PSPIN)
        JFMAX=FJMAX
        FJMAX1=JFMAX
        IF(FJMAX-FJMAX1)88,44,45
   44   FJ=0.0
        FJI=0.0
        NCOE=FJMAX+1.
  303   WRITE OUTPUT TAPE KTAPE, 203,NTL
  203   FORMAT(1H0,10X,27HOUTPUT WILL BE INTEGER FOR I2,19H INPUT VALUES O
       1F TL,/)
        GO TO 46
   45   FJ=0.5
        FJI=0.5
        NCOE=FJMAX+.5
        WRITE OUTPUT TAPE KTAPE, 204,NTL
  204   FORMAT(1H0,10X,32HOUTPUT WILL BE HALF-INTEGER FOR I2,19H INPUT VAL
       1UES OF TL,/)
   46   K=1
   47   S=SLL
   16   SU=ABSF(FJ+S)
        SL=ABSF(FJ-S)
```

```
      SL=SL+1.
      SU=SU+1.
       TLNDX=SL
      SUM=0.0
   48 I=TLNDX
      IF(TL(I))148,49,148
  148 SUM=SUM+((2.*FJ+1.)/C)*TL(I)
      IF(TLNDX-SU)17,49,49
   17 TLNDX=TLNDX+1.
      GO TO 48
   49 CS(K)=CS(K)+SUM*PORPC
      S=S+1.
      IF(S-SUL)16,16,50
   50 IF(FJ-FJMAX)51,52,52
   51 FJ=FJ+1.
      K=K+1
      GO TO 47
   52 SUMJC=0.0
      DO 53 I=1,200
   53 SUMJC=SUMJC+CS(I)
      SUMJ=0.0
      FJ1=FJI
      DO 54 I=1,200
      PJC(I)=CS(I)/SUMJC
      FJ2=FJ1*FJ1
      SUMJ=SUMJ+PJC(I)*FJ2
   54 FJ1=FJ1+1.
      FJ1=FJI
      SUM=0.0
      WRITE OUTPUT TAPE KTAPE,1113
 1113 FORMAT(1HO,3H  L,15X,2HTL,13X,2HJC,5X,13HCROSS SECTION,12X,3HPJC,1
     14X,9HSUM   PJC,10X,13H(JC)(JC) AVE.///)
      FJIX=0.0
      SUM=SUM+PJC(1)
      WRITE OUTPUT TAPE KTAPE,1114,FJIX,TL(1),FJ1,CS(1),PJC(1),SUM,SUMJ
 1114 FORMAT(1H ,1X,F4.1,5X,E15.8,5X,F4.1,4(5X,E15.8))
      DO 14 I=2,NTL
      FJIX=FJIX+1.
      FJ1=FJ1+1.
      SUM=SUM+PJC(I)
   14 WRITE OUTPUT TAPE KTAPE,1115,FJIX,TL(I),FJ1,CS(I),PJC(I),SUM
 1115 FORMAT(1H ,1X,F4.1,5X,E15.8,5X,F4.1,3(5X,E15.8))
      I=NTL+1
      FJ1=FJ1+1.
   15 IF(FJ1-FJMAX)412,412,411
  412 SUM=SUM+PJC(I)
      WRITE OUTPUT TAPE KTAPE,1116,FJ1,CS(I),PJC(I),SUM
      WRITE OUTPUT TAPE 6,1116,FJ1,CS(I),PJC(I),SUM
 1116 FORMAT(1H ,30X,F4.1,3(5X,E15.8))
      I=I+1
      FJ1=FJ1+1.
      GO TO 15
  411 GO TO(1001,88,88,1200, 88 ,1200),MPD
C
C     NORMALIZED  SPIN  DISTRIBUTION  FOLLOWING  PARTICLE  EMISSION
C
 1200 NPE1=1
      CJC=FJMAX
      NJC=NCOE
      DO 1301 I=1,200
      TL(I)=0.
      CS(I)=0.
```

```
1301 PJF(I)=0.
     READ 99,NPE
     GOTO 808
1000 READ 99,NPE
 111 FORMAT(F6.3)
 889 READ 99,NJC
  99 FORMAT(I2)
     DO 2 I=1,NJC
   2 READ 990,PJC(I),CJC
     NPE1=1
 808 READ 111,SP
 888 READ 99,NTL
      DO 31 I=1,NTL
  31 READ 990,TL(I),CL
 990 FORMAT(E15.8,5X,F4.1)
 893 READ 111,SIGMA
     FJMAX=CL+CJC+SP
     CJMAX=CJC
     L=1
     SUM=0.
     B1=0.
     WRITE OUTPUT TAPE KTAPE, 113
 113 FORMAT(1H1,15X,56HNORMALIZED SPIN DISTRIBUTION FOLLOWING PARTICLE
    1EMISSION//)
     WRITE OUTPUT TAPE KTAPE, 109
     WRITE OUTPUT TAPE KTAPE, 890,NPE1
 890 FORMAT(1H0,30X,33HDISTRIBUTION  FOR  PARTICLE  NO. I2,/)
     WRITE OUTPUT TAPE KTAPE, 114,SIGMA
     WRITE OUTPUT TAPE KTAPE, 118,SP
 114 FORMAT(1H0,24X,19HINPUT  SIGMA  WAS  E15.8)
     WRITE OUTPUT TAPE 6, 118, SP
 118 FORMAT(1H0,24X,25HOUTGOING  PARTICLE  SPIN=F6.4)
     WRITE OUTPUT TAPE KTAPE, 115,FJMAX
 115 FORMAT(1H0,24X,25HJFMAX=LMAX+JCMAX+S PRIME=F7.4)
     JMAX=FJMAX
     FJMAX1=JMAX
     IF(FJMAX-FJMAX1)88,3,4
   3 FJI=0 .
     CJI=0.5
     CJ=.5
     FJ=0.
     FJII=0.
     NCOE=FJMAX+1.
     WRITE OUTPUT TAPE KTAPE, 116,NTL
 116 FORMAT(1H0,24X,31HOUTPUT  WILL  BE  INTEGER  FOR I2,22H INPUT  VAL
    1UES  OF  TL,/)
     GO TO 55
   4 FJI=.5
     CJI=0.
     CJ=0.
     FJ=.5
     FJII=0.5
     NCOE=FJMAX+.5
     WRITE OUTPUT TAPE KTAPE, 117,NTL
 117 FORMAT(1H0,24X,36HOUTPUT  WILL  BE  HALF-INTEGER  FOR I2,22H INPUT
    1  VALUES  OF  TL,/)
  55 FJN=FJ
     FCT=FJN+CL+SP
     FCL=FJN-CL-SP
     IF(FCL)666,667,667
 666 CJ=CJI
     GO TO 668
```

```
  667 CJ=FCL
  668 IF(CJMAX-FCT) 2667,2667,2668
 2667 FCT=CJMAX
      GO TO 2668
 2668 K=CJ+1.
      NOD=1
    5 SUMTL=0.0
      SU=ABSF(FJN+SP)
      SL=ABSF(FJN-SP)
      S=SL
   11 UL=ABSF(CJ+S)+1.
      BL=ABSF(CJ-S)+1.
      TDX=BL
  110 I=TDX
      IF(TL(I))87,7,87
   87 SUMTL=SUMTL+TL(I)
      IF(TDX-UL)6,7,7
    6 TDX=TDX+1.
      GO TO110
    7 IF(S-SU)8,9,9
    8 S=S+1.
      GO TO 11
    9 GO TO (669,665),NOD
  669 FJN=FJ
  665 ARG=-((FJN+.5)**2.)/(2.*SIGMA*SIGMA)
      TEMP= (SUMTL*EXPF(ARG))*(2.*FJN+1.)
      GOTO(551,552),NOD
  551 T=TEMP
      NOD=2
      FJT=CJ+CL+SP
      FJL=CJ-CL-SP
       IF(FJL)461,462,462
  461 FJN=FJI
      GOTO 5
  462 FJN=FJL
      GOTO 5
  552 B1=B1+TEMP
      IF(FJN-FJT)557,558,558
  557 FJN=FJN+1.
      GO TO 5
  558 IF(B1) 1558,1559,1558
 1558 CS(L)=CS(L)+(T/B1)*PJC(K)
 1559 B1=0.
      IF(FCT-CJ)560,560,559
  559 K=K+1
   10 CJ=CJ+1.
      NOD=1
      FJN=FJ
      GO TO 5
  560 SUM=SUM+CS(L)
      IF(FJMAX-FJ)570,570,561
  561 L=L+1
      FJ=FJ+1.
   13 CJ=CJI
      GO TO 55
  570 FJ=FJI
      AVE=0.
      DO 77 I=1,L
      PJF(I)=CS(I)/SUM
      AVE=PJF(I)*FJ*FJ+AVE
   77 FJ=FJ+1.
      SUM=0.
```

```
      I=1
      FJ=FJII
      CJ=CJI
      WRITE OUTPUT TAPE KTAPE, 401
  401 FORMAT(1H0,2H L,13X,2HTL,11X,2HJC,11X,3HPJC,12X,2HJF,11X,3HPJF,13X
     1,9HSUM    PJF, 9X,13H(JF)(JF) AVE.)
      AI=I-1
      SUM=SUM+PJF(I)
      WRITE OUTPUT TAPE KTAPE, 402,AI,TL(1),CJ,PJC(1),FJ,PJF(1),SUM,AVE
  402 FORMAT(1H0,F4.1,4X,E15.8,4X,F4.1,4X,E15.8,4X,F4.1,3(4X,E15.8))
      DO 66 I=2,NTL
      CJ=CJ+1.
      FJ=FJ+1.
      SUM=SUM+PJF(I)
      AI=I-1
   66 WRITE OUTPUT TAPE KTAPE, 403,AI,TL(I),CJ,PJC(I),FJ,PJF(I),SUM
  403 FORMAT(1H ,F4.1,4X,E15.8,4X,F4.1,4X,E15.8,4X,F4.1, 2(4X,E15.8))
      N=I
      DO 67 I=N,NJC
      FJ=FJ+1.
      CJ=CJ+1.
      SUM=SUM+PJF(I)
   67 WRITE OUTPUT TAPE KTAPE, 404,CJ,PJC(I),FJ,PJF(I),SUM
  404 FORMAT(1H ,27X,F4.1,4X,E15.8,4X,F4.1,2(4X,E15.8))
      I=NJC+1
 1462 FJ=FJ+1.
      IF(FJ-FJMAX)413,413,414
  413 SUM=SUM+PJF(I)
   68 WRITE OUTPUT TAPE KTAPE, 405,FJ,PJF(I),SUM
  405 FORMAT(1H ,54X,F4.1,2(4X,E15.8))
      I=I+1
      GO TO 1462
  414 IF(NPE-NPE1)891,891,892
  892 NPE1=NPE1+1
      CJC=FJMAX
      NJC=NOCE
      DO 894 I=1,200
      TL(I)=0.
      CS(I)=0.
      PJC(I)=PJF(I)
  894 PJF(I)=0.
      GO TO 888
  891 GO TO(88,1001,88,1001,9000,9000),NPD
   88 STOP
C
C     NORMALIZED  SPIN  DISTRIBUTION  FOLLOWING  GAMMA-RAY  EMISSION
C
 9000 NFJI=NOCE
      CJI=FJMAX
      DO 246 I=1,200
      FJFS(I)=0.
      RHO(I)=0.
  246 FJI(I)=PJF(I)
      GO TO 9002
 9001 READ 99,NFJI
      DO 142 I=1,NFJI
  142 READ 99C,FJI(I),CJI
 9002 NGC=1
      READ 99,NGE
   98 READ 111,SIGMA
      READ 99,L
      WRITE OUTPUT TAPE KTAPE, 776,NGC
```

```
  776 FORMAT(1H1,24X,72HNORMALIZED  SPIN  DISTRIBUTION  FOLLOWING  EMISS
     1ION  OF  GAMMA  RAY  NO.  I2,//)
      WRITE OUTPUT TAPE KTAPE, 109
      WRITE OUTPUT TAPE KTAPE, 778,SIGMA
  778 FORMAT(1H0,24X,24HSPIN  CUT  OFF  FACTOR = F6.3)
      CL=L
      WRITE OUTPUT TAPE KTAPE, 775,L
  775 FORMAT(1H0,24X,39HMULTIPOLARITY  OF  GAMMA-RAY  EMISSION I2)
      FJMAX=CL+CJI
      WRITE OUTPUT TAPE KTAPE,7779,FJMAX
 7779 FORMAT(1H0,24X, 18HJF(MAX)=JI(MAX)+L=F6.3)
      J=CJI
      CJ=J
      I=0
      IF(CJI-CJ)133,134,133
  133 FJ1=.5
      GO TO 155
  134 FJ1=0.
  155 FJ=FJ1
  255 I=I+1
      ARG=-(((FJ+.5)**2.)/(2.*SIGMA*SIGMA))
      RHO(I)=(2.*FJ+1.)*EXPF(ARG)
      FJ=FJ+1.
      IF(FJ-FJMAX-2.*CL)255,255,256
  256 FJS=FJ1
      J=1
  372 ULL=FJS+CL
       BLL=ABSF(FJS-CL)
      CJ=BLL
      IF(FJ1)88,1813,1812
 1813 JI=CJ
      GO TO 375
 1812 JI=CJ-.5
  375 FML=CJ+CL
      FLL=ABSF(CJ-CL)
      CI=FLL
      IF(FJ1)88,1814,1815
 1814 I=CI
      GO TO 1816
 1815 I=CI-.5
 1816 SUM=0.0
  370 SUM=SUM+RHO(I+1)
      I=I+1
      CI=CI+1.
      IF(FML-CI)371,370,370
  371 IF(SUM) 1371,1372,1371
 1371 FJFS(J)=FJFS(J)+(FJI(JI+1)*RHO(J    )/SUM)
 1372 CJ=CJ+1 .
      JI=JI+1
      IF(ULL-CJ)373,375,375
  373 J=J+1
       FJS=FJS+1.
      IF(FJMAX-FJS)374,372,372
  374 FJ=FJ1
      FSUM=0.
      AVE=0.
      DO 222 I=1,J
      AVE=FJ*FJ*FJFS(I) +AVE
  222 FJ=FJ+1.
      JJ=FJMAX+1.
      I=1
      SUM=0.
```

```
      WRITE OUTPUT TAPE KTAPE, 780
  780 FORMAT(1HO,5X,2HJI,13X,3HJFI,17X,2HJF,13X,3HFJF,17X,9HSLM    FJF,12
     1X,13H(JF)(JF) AVE.)
      SUM=SUM+FJFS(I)
      FJ=FJ1
      WRITE OUTPUT TAPE KTAPE, 781,FJ,FJI(I),FJ,FJFS(I),SUM,AVE
  781 FORMAT(1HO,4X,F4.1,7X,E15.8,9X,F4.1,3(7X,E15.8))
      IF(NFJI-1) 88,1264,1263
 1263 DO 263 I=2,NFJI
      FJ=FJ+1.
      SUM=SUM+FJFS(I)
  263 WRITE OUTPUT TAPE KTAPE, 782,FJ,FJI(I),FJ,FJFS(I),SUM
  782 FORMAT(1H ,4X,F4.1,7X,E15.8,9X,F4.1,2(7X,E15.8))
 1264 FJ=FJ+1.
      I=NFJI+1
  150 SUM=SUM+FJFS(I)
      WRITE OUTPUT TAPE KTAPE, 783,FJ,FJFS(I),SUM
  783 FORMAT(1H ,   39X,F4.1,2(7X,E15.8) )
      I=I+1
      FJ=FJ+1.
      IF(FJMAX-FJ)140,150,150
  140 NGE=NGE-1
      NGC=NGC+1
      IF(NGE-1) 19,18,18
   18 DO 166 I=1,200
      FJI(I)=FJFS(I)
      RHO(I)=0.
  166 FJFS(I)=0.
      NFJI=NFJI+1
      CJI=FJMAX
      GO TO 98
   19 GO TO 1001

      END(0,1,0,0,1)
```

PA234 CS ISOMER RATIO FERMI GAS MODEL TRY 2 J=11

DISTRIBUTION FOR PARTICLE NO. 1

INPUT SIGMA WAS 7.08000000E 00

OUTGOING PARTICLE SPIN= .5000

OUTGOING PARTICLE SPIN= .5000

JFMAX=LMAX+JCMAX+S PRIME=44.5000

OUTPUT WILL BE HALF-INTEGER FOR 11 INPUT VALUES OF TL

L	TL	JC	PJC	JF	PJF	SUM PJF	
0	8.35161000E-01	0	8.24205000E-03	.5	8.31028823E-03	8.31028823E-03	1.
1.0	3.83010000E-01	1.0	2.43208000E-02	1.5	2.73612319E-02	3.56715201E-02	
2.0	9.91382000E-01	2.0	3.92165900E-02	2.5	4.72128048E-02	8.28843249E-02	
3.0	8.03900000E-02	3.0	5.22471500E-02	3.5	6.12936825E-02	1.44178007E-01	
4.0	1.01545000E-01	4.0	6.28772300E-02	4.5	7.16805826E-02	2.15858590E-01	
5.0	5.90000000E-04	5.0	7.07540700E-02	5.5	7.81426871E-02	2.94001277E-01	
6.0	1.04000000E-04	6.0	7.57236600E-02	6.5	8.13801707E-02	3.75381448E-01	
7.0	1.00000000E-06	7.0	7.78270400E-02	7.5	8.15934029E-02	4.56964851E-01	
8.0	0E 00	8.0	7.72788800E-02	8.5	7.91150166E-02	5.36079867E-01	
9.0	0E 00	9.0	7.44320100E-02	9.5	7.44620173E-02	6.10541885E-01	
10.0	0E 00	10.0	6.97334600E-02	10.5	6.81804962E-02	6.78722381E-01	
		11.0	6.36776600E-02	11.5	6.08409835E-02	7.39563364E-01	
		12.0	5.67620700E-02	12.5	5.29811355E-02	7.92544500E-01	
		13.0	4.94495700E-02	13.5	4.50697276E-02	8.37614227E-01	
		14.0	4.21404200E-02	14.5	3.74838232E-02	8.75098050E-01	
		15.0	3.51549300E-02	15.5	3.04990134E-02	9.05597064E-01	
		16.0	2.87265700E-02	16.5	2.42910420E-02	9.29888106E-01	
		17.0	2.30040700E-02	17.5	1.89461156E-02	9.48834221E-01	
		18.0	1.80603800E-02	18.5	1.44767680E-02	9.63310989E-01	
		19.0	1.39059200E-02	19.5	1.08402456E-02	9.74151235E-01	
		20.0	1.05039000E-02	20.5	7.95685097E-03	9.82108086E-01	
		21.0	7.78553000E-03	21.5	5.72637916E-03	9.87834465E-01	
		22.0	5.66379000E-03	22.5	4.04151716E-03	9.91875982E-01	
		23.0	4.04472000E-03	23.5	2.79776883E-03	9.94673751E-01	
		24.0	2.83599000E-03	24.5	1.89998657E-03	9.96573738E-01	
		25.0	1.95262000E-03	25.5	1.26596284E-03	9.97839700E-01	
		26.0	1.32034000E-03	26.5	8.27707192E-04	9.98667408E-01	
		27.0	8.76910000E-04	27.5	5.31087100E-04	9.99198495E-01	
		28.0	5.72100000E-04	28.5	3.34446243E-04	9.99532941E-01	
		29.0	3.66670000E-04	29.5	2.06715449E-04	9.99739656E-01	

NORMALIZED SPIN DISTRIBUTION FOLLOWING PARTICLE EMISSION

PA?34 CS ISOMER RATIO FERMI GAS MODEL TRY 2 J=11

DISTRIBUTION FOR PARTICLE NO. 2

INPUT SIGMA WAS 5.00000000E 00

OUTGOING PARTICLE SPIN= .5000

OUTGOING PARTICLE SPIN= .5000

JFMAX=LMAX+JCMAX+S PRIME=55.0000

OUTPUT WILL BE INTEGER FOR 11 INPUT VALUES OF TL

L	TL	JC	PJC	JF	PJF	SUM PJF	(J
0	8.23238000E-01	.5	8.31028823E-03	0	1.84510141E-03	1.84510141E-03	9.75
1.0	3.83144000E-01	1.5	2.73612319E-02	1.0	1.52361837E-02	1.70812852E-02	
2.0	9.83065000E-01	2.5	4.72128048E-02	2.0	3.60307369E-02	5.31120220E-02	
3.0	8.10710000E-02	3.5	6.12936825E-02	3.0	5.67317192E-02	1.09843741E-01	
4.0	9.80420000E-02	4.5	7.16805826E-02	4.0	7.26761823E-02	1.82519923E-01	
5.0	5.64300900E-04	5.5	7.81426871E-02	5.0	8.27600440E-02	2.65279967E-01	
6.0	1.07000000E-04	6.5	8.13801707E-02	6.0	8.76655958E-02	3.52945563E-01	
7.0	1.00100900E-06	7.5	8.15834029E-02	7.0	8.83779507E-02	4.41323514E-01	
8.0	0E 00	8.5	7.91150166E-02	8.0	8.56725846E-02	5.26996099E-01	
9.0	0E 00	9.5	7.44620173E-02	9.0	8.02948031E-02	6.07290902E-01	
10.0	0E 00	10.5	6.81804962E-02	10.0	7.29774008E-02	6.80268302E-01	
		11.5	6.08409835E-02	11.0	6.44543581E-02	7.44722661E-01	
		12.5	5.29811355E-02	12.0	5.54044769E-02	8.00127137E-01	
		13.5	4.50697276E-02	13.0	4.64065227E-02	8.46533660E-01	
		14.5	3.74838232E-02	14.0	3.79104498E-02	8.84444110E-01	
		15.5	3.04990134E-02	15.0	3.02279795E-02	9.14672089E-01	
		16.5	2.42910420E-02	16.0	2.35393518E-02	9.38211441E-01	
		17.5	1.89461156E-02	17.0	1.79116053E-02	9.56123047E-01	
		18.5	1.44767680E-02	18.0	1.33233451E-02	9.69446392E-01	
		19.5	1.08402456E-02	19.0	9.69141371E-03	9.79137805E-01	
		20.5	7.95685097E-03	20.0	6.89588862E-03	9.86033694E-01	
		21.5	5.72637916E-03	21.0	4.80107947E-03	9.90834773E-01	
		22.5	4.04151716E-03	22.0	3.27140917E-03	9.94106183E-01	
		23.5	2.79776883E-03	23.0	2.13206650E-03	9.96288249E-01	
		24.5	1.89998657E-03	24.0	1.42500974E-03	9.97713259E-01	
		25.5	1.26596284E-03	25.0	9.11284282E-04	9.98624543E-01	
		26.5	8.27707192E-04	26.0	5.70601679E-04	9.99195145E-01	
		27.5	5.31087100E-04	27.0	3.49639073E-04	9.99544784E-01	

NORMALIZED SPIN DISTRIBUTION FOLLOWING EMISSION OF GAMMA RAY NO. 1

PA234 CS ISOMER RATIO FERMI GAS MODEL TRY 2 J=11

SPIN CUT OFF FACTOR = 5.260

MULTIPOLARITY OF GAMMA-RAY EMISSION 1

JF(MAX)=JI(MAX)+L=56.000

JI	JFI	JF	FJF	SUM FJF	(JF)(JF)
0	1.84510141E-03	0	1.81822236E-03	1.81822236E-03	9.47329493
1.0	1.52361837E-02	1.0	1.51165160E-02	1.69347383E-02	
2.0	3.60307368E-02	2.0	3.61034107E-02	5.30381490E-02	
3.0	5.67317192E-02	3.0	5.74822757E-02	1.10520425E-01	
4.0	7.26761823E-02	4.0	7.42713800E-02	1.84791805E-01	
5.0	8.27600440E-02	5.0	8.43966023E-02	2.69688407E-01	
6.0	8.76655958E-02	6.0	8.93762948E-02	3.59564702E-01	
7.0	8.83779507E-02	7.0	9.02691059E-02	4.49833808E-01	
8.0	8.56725846E-02	8.0	8.70536428E-02	5.36887450E-01	
9.0	8.02948031E-02	9.0	8.10848839E-02	6.17972334E-01	
10.0	7.29774008E-02	10.0	7.31886632E-02	5.91160997E-01	
11.0	6.44543581E-02	11.0	6.41539138E-02	7.55314911E-01	
12.0	5.54044769E-02	12.0	5.46958862E-02	8.10010797E-01	
13.0	4.64065227E-02	13.0	4.54105495E-02	8.55421347E-01	
14.0	3.79104498E-02	14.0	3.67484754E-02	8.92169822E-01	
15.0	3.02279795E-02	15.0	2.90090113E-02	9.21178834E-01	
16.0	2.35393518E-02	16.0	2.23516077E-02	9.43530441E-01	
17.0	1.79116053E-02	17.0	1.68187142E-02	9.60349156E-01	
18.0	1.33233451E-02	18.0	1.23644794E-02	9.72713635E-01	
19.0	9.69141371E-03	19.0	8.88425721E-03	9.81597892E-01	
20.0	6.89588862E-03	20.0	6.24122526E-03	9.87839117E-01	
21.0	4.80107947E-03	21.0	4.28790843E-03	9.92127026E-01	
22.0	3.27140917E-03	22.0	2.88175515E-03	9.95008781E-01	
23.0	2.18206650E-03	23.0	1.89496667E-03	9.96903748E-01	
24.0	1.42500974E-03	24.0	1.21945322E-03	9.98123201E-01	
25.0	9.11284282E-04	25.0	7.68024085E-04	9.98891225E-01	
26.0	5.70601679E-04	26.0	4.73287941E-04	9.99364513E-01	
27.0	3.49639073E-04	27.0	2.84910737E-04	9.99649324E-01	
28.0	2.08883740E-04	28.0	1.66543651E-04	9.99815867E-01	
29.0	1.20770065E-04	29.0	9.35660173E-05	9.99909433E-01	
30.0	6.64422582E-05	30.0	4.96020170E-05	9.99959035E-01	
31.0	3.39661995E-05	31.0	2.42463087E-05	9.99983282E-01	
32.0	1.56908294E-05	32.0	1.06707106E-05	9.99993952E-01	
33.0	6.37664479E-06	33.0	4.13957713E-06	9.99998092E-01	
34.0	2.22983716E-06	34.0	1.39012660E-06	9.99999482E-01	
35.0	6.57283137E-07	35.0	3.93485996E-07	9.99999881E-01	

NORMALIZED SPIN DISTRIBUTION FOLLOWING EMISSION OF GAMMA RAY NO. 2

PA234 CS ISOMER RATIO FERMI GAS MODEL TRY 2 J=11

SPIN CUT OFF FACTOR = 4.988

MULTIPOLARITY OF GAMMA-RAY EMISSION 1

JF(MAX)=JI(MAX)+L=57.000

JI	JFI	JF	FJF	SUM FJF	(JF)(JF)
0	1.81822236E-03	0	1.81823243E-03	1.81823243E-03	9.1548502
1.0	1.51165160E-02	1.0	1.51776015E-02	1.69958339E-02	
2.0	3.61034107E-02	2.0	3.65151529E-02	5.35109868E-02	
3.0	5.74822757E-02	3.0	5.86021816E-02	1.12113168E-01	
4.0	7.42713800E-02	4.0	7.61854329E-02	1.88298601E-01	
5.0	8.48966023E-02	5.0	8.73083741E-02	2.75606975E-01	
6.0	8.98762948E-02	6.0	9.23053968E-02	3.67912372E-01	
7.0	9.02691059E-02	7.0	9.23153402E-02	4.60227712E-01	
8.0	8.70536429E-02	8.0	8.84829212E-02	5.48710634E-01	
9.0	8.10848839E-02	9.0	8.18202342E-02	6.30530868E-01	
10.0	7.31886632E-02	10.0	7.32537241E-02	7.03784592E-01	
11.0	6.41539138E-02	11.0	6.36416967E-02	7.67426289E-01	
12.0	5.46958862E-02	12.0	5.37386223E-02	8.21164911E-01	
13.0	4.54105495E-02	13.0	4.41562579E-02	8.65321169E-01	
14.0	3.67484754E-02	14.0	3.53408870E-02	9.00662056E-01	
15.0	2.90090113E-02	15.0	2.75728460E-02	9.28234902E-01	
16.0	2.23516077E-02	16.0	2.09838507E-02	9.49218752E-01	
17.0	1.68187142E-02	17.0	1.55856065E-02	9.64804359E-01	
18.0	1.23644794E-02	18.0	1.13031048E-02	9.76107464E-01	
19.0	8.88425721E-03	19.0	8.00719643E-03	9.84114660E-01	
20.0	6.24122526E-03	20.0	5.54272276E-03	9.89657383E-01	
21.0	4.28790843E-03	21.0	3.75024280E-03	9.93407626E-01	
22.0	2.88175515E-03	22.0	2.48089452E-03	9.95888520E-01	
23.0	1.89496667E-03	23.0	1.60500581E-03	9.97493526E-01	
24.0	1.21945322E-03	24.0	1.01562990E-03	9.98509156E-01	
25.0	7.64124085E-04	25.0	6.28589999E-04	9.99137746E-01	
26.0	4.73287941E-04	26.0	3.80113586E-04	9.99517859E-01	
27.0	2.94810737E-04	27.0	2.23863100E-04	9.99741723E-01	
28.0	1.66543651E-04	28.0	1.27407488E-04	9.99869130E-01	
29.0	9.35660173E-05	29.0	6.91222267E-05	9.99938252E-01	
30.0	4.96020170E-05	30.0	3.50748670E-05	9.99973327E-01	
31.0	2.42463087E-05	31.0	1.62965417E-05	9.99989624E-01	
32.0	1.06707106E-05	32.0	6.79478547E-06	9.99996418E-01	
33.0	4.13957713E-06	33.0	2.49863263E-06	9.99998917E-01	
34.0	1.39012660E-06	34.0	7.99267063E-07	9.99999716E-01	

NORMALIZED SPIN DISTRIBUTION FOLLOWING EMISSION OF GAMMA RAY NO. 3

PA234 CS ISOMER RATIO FERMI GAS MODEL TRY 2 J=11

SPIN CUT OFF FACTOR = 4.660

MULTIPOLARITY OF GAMMA-RAY EMISSION 1

JF(MAX)=JI(MAX)+L=58.000

JI	JFI	JF	FJF	SUM FJF	(JF)(JF)
0	1.81823243E-03	0	1.84646278E-03	1.84646278E-03	9.78755644
1.0	1.51776015E-02	1.0	1.54575509E-02	1.73040137E-02	
2.0	3.65151529E-02	2.0	3.73645599E-02	5.46685836E-02	
3.0	5.86021816E-02	3.0	6.02711027E-02	1.14939686E-01	
4.0	7.61854329E-02	4.0	7.86349124E-02	1.93574599E-01	
5.0	8.73083741E-02	5.0	9.01725753E-02	2.83747174E-01	
6.0	9.23053968E-02	6.0	9.50766435E-02	3.78823818E-01	
7.0	9.23153402E-02	7.0	9.45613546E-02	4.73385172E-01	
8.0	8.84829212E-02	8.0	8.99551392E-02	5.63340311E-01	
9.0	8.18202342E-02	9.0	8.24430203E-02	6.45783332E-01	
10.0	7.32537241E-02	10.0	7.30792832E-02	7.18862615E-01	
11.0	6.36416967E-02	11.0	6.29024057E-02	7.81665021E-01	
12.0	5.37386223E-02	12.0	5.24102157E-02	8.34075236E-01	
13.0	4.41562579E-02	13.0	4.25262177E-02	8.76601454E-01	
14.0	3.53408870E-02	14.0	3.35839375E-02	9.10185391E-01	
15.0	2.75728460E-02	15.0	2.58341669E-02	9.36019558E-01	
16.0	2.09838507E-02	16.0	1.93704876E-02	9.55390046E-01	
17.0	1.55856065E-02	17.0	1.41651244E-02	9.69555170E-01	
18.0	1.13031048E-02	18.0	1.01076398E-02	9.79662810E-01	
19.0	8.00719643E-03	19.0	7.04071930E-03	9.86703529E-01	
20.0	5.54272276E-03	20.0	4.78948375E-03	9.91493013E-01	
21.0	3.75024230E-03	21.0	3.18283025E-03	9.94675843E-01	
22.0	2.48089452E-03	22.0	2.06692713E-03	9.96742771E-01	
23.0	1.60500581E-03	23.0	1.31199347E-03	9.98054764E-01	
24.0	1.01562990E-03	24.0	8.14102078E-04	9.98868866E-01	
25.0	6.28589899E-04	25.0	4.93554794E-04	9.99362421E-01	
26.0	3.80113585E-04	26.0	2.91739545E-04	9.99654160E-01	
27.0	2.23863100E-04	27.0	1.67213903E-04	9.99821374E-01	
28.0	1.27407488E-04	28.0	9.13607452E-05	9.99913335E-01	
29.0	6.91222675E-05	29.0	4.77678441E-05	9.99961103E-01	
30.0	3.50748670E-05	30.0	2.29946479E-05	9.99984098E-01	
31.0	1.62965417E-05	31.0	1.00640450E-05	9.99994162E-01	
32.0	6.79478547E-06	32.0	3.93712335E-06	9.99998099E-01	
33.0	2.49863263E-06	33.0	1.35780149E-06	9.99999457E-01	
34.0	7.99267063E-07	34.0	4.08279063E-07	9.99999865E-01	